LBNL-42351

EOS9nT: A TOUGH2 MODULE FOR THE SIMULATION OF WATER FLOW AND SOLUTE /COLLOID TRANSPORT IN THE SUBSURFACE

George J. Moridis, Yu-Shu Wu and Karsten Pruess

Earth Sciences Division
Lawrence Berkeley National Laboratory
Berkeley, CA 94720

March 1999

This work was supported by the Director, Office of Civilian Radioactive Waste Management, U.S. Department of Energy, through Memorandum Purchase Order EA9013MC5X between TRW Environmental Safety Systems and the Ernest Orlando Lawrence Berkeley National Laboratory (Berkeley Lab). The support is provided to Berkeley Lab through the U.S. Department of Energy Contract No. DE-AC03-76SF00098.

DISCLAIMER

DISCLAIMER

Portions of this document may be illegible in electronic image products. Images are produced from the best available original document.

EOS9nT: A TOUGH2 Module for the Simulation of Water Flow and Solute/Colloid Transport in the Subsurface

George J. Moridis, Yu-Shu Wu and Karsten Pruess
Earth Sciences Division, Lawrence Berkeley National Laboratory,University of California, Berkeley, California

Abstract

EOS9nT is a new TOUGH2 module for the simulation of flow and transport of an arbitrary number n of non-volatile tracers (solutes and/or colloids) in the subsurface. The module first solves the Richards equation, which describes saturated or unsaturated water flow in subsurface formations, and obtains the flow regime. A second set of transport equations, corresponding to the n tracers/colloids, are then solved sequentially. The very low concentrations of the n tracers are considered to have no effect on the density of the liquid phase, thus making possible the decoupling of the transport from the flow equations.

The n tracer transport equations account for sorption, radioactive decay, advection, hydrodynamic dispersion, molecular diffusion, filtration (for colloids only), first-order chemical reactions, and colloid-assisted tracer transport. A total of $n-1$ daugter products of radioactive decay can be tracked. EOS9nT can handle gridblocks of irregular geometry in 3-D domains, and offers the option of a Laplace space formulation of the transport equations (in addition- to conventional timestepping) after the flow field becomes time-invariant. The Laplace transform formulation eliminates the need for time discretization and the problems stemming from the treatment of the time derivatives in the transport equations, and yields solutions semi-analytical in time. An unlimited time step size is thus possible without loss of accuracy.

In this report we discuss the mathematical basis of the processes and phenomena simulated by EOS9nT, and provide a user's manual for the implementation of the module. The performance of the module is verified by using several verification problems, which show an excellent agreement between the numerical predictions and the known analytical solutions.

1. Introduction

EOS9nT is a module for the TOUGH2 general-purpose fluid and heat flow simulator [*Pruess*, 1991]. It is designed to simulate the flow of water and the transport of an arbitrary number n of independent tracers (**S**olutes and/or **C**olloids, SCs) in complex subsurface systems involving porous and/or fractured media. EOS9nT can simulate the isothermal flow of the aqueous phase, and SC transport at concentrations too low to have any measurable effect on the water properties and the flow regime.

The current version is an extension of an earlier EOS9nT version [*Moridis et al.*, 1998], and includes two types of Laplace transform formulations of the SC equations in addition to conventional timestepping. The Laplace transform allows an unlimited timestep size without loss of accuracy or stability. For tracer transport simulation involving coupled-process capabilities (non-isothermal and/or variable density), the reader is referred to the companion EOS3nT module [*Moridis et al.*, 1999].

2. Governing Equations

2.1. Modeled Processes and Underlying Assumptions

EOS9nT can model

(1) the flow of the liquid phase under saturated and/or unsaturated conditions under constant fluid density and viscosity conditions, and

(2) the transport of an arbitrary number n of SCs, accounting for

   (a) advection,

   (b) molecular diffusion,

   (c) hydrodynamic dispersion (with full 3-D tensorial representation),

   (d) equilibrium, kinetic or combined sorption (physical and/or chemical), following linear, Langmuir and/or Freundlich isotherms,

   (e) radioactive decay,

   (f) tracking up to $n-1$ daughter products of radioactive decay or reaction products,

   (g) linear chemical reactions,

(h) filtration (for colloids only), and

(i) colloid-assisted solute transport.

The flow component in EOS9nT is based on the EOS9 module [*Wu et al.*, 1996; *Wu and Mishra*, 1998], in which a single equation is solved. This is the *Richards* [1931] equation, which describes the flow of water in the subsurface under saturated or unsaturated conditions under the following assumptions:

1. The water flow is isothermal.
2. The concentration of the SCs is at a tracer level, i.e., too low to have any measurable effect on the flow regime.
3. The pressure of the gaseous phase does not deviate significantly from the reference pressure of the system.
4. There is no phase change.

These assumptions allow decoupling of the flow and transport equations. The Richards equation is first solved, followed by the sequential solution of the n independent tracer transport equations. If any combination of assumptions (1), (2) and (4) does not hold true, then the companion EOS3nT module [*Moridis et al.*, 1999] must be used.

2.2. The Water Equation

Following *Pruess* [1987; 1991], mass balance considerations in every subdomain (gridblock) into which the flow domain has been subdivided by the integral finite difference method dictates that

$$\frac{d}{dt}\int_{V_n} M_\kappa \, dV = \int_{\Gamma_n} \mathbf{F}_\kappa \cdot \mathbf{n} \, d\Gamma + \int_{V_n} q_\kappa \, dV \,, \tag{1}$$

where

V, V_n volume, volume of subdomain n [L^3];

M_κ mass accumulation term of component κ $[ML^{-3}]$;

Γ, Γ_n surface area, surface area of subdomain n $[L^2]$;

$\mathbf{F}_\kappa$ Darcy flux vector of component κ $[ML^{-2}T^{-1}]$;

$\mathbf{n}$ inward unit normal vector $[L^0]$;

q_κ source/sink term of component κ $[ML^{-3}T^{-1}]$;

t time $[T]$.

For water ($\kappa \equiv w$), the mass accumulation term M in equation (1) is given by

$$M_w = \phi \; S_w \; \rho \; , \tag{2}$$

where

ϕ porosity $[L^3L^{-3}]$;

ρ water density $[ML^{-3}]$;

S_w water saturation $[L^0]$.

The water flux term is given by

$$\mathbf{F}^w = \sum_m A_{nm} F_{nm} = \sum_m A_{nm} \left(\frac{k \; k_{rw} \; \rho_w}{\mu_w} \right)_{nm} \left(\frac{P_n - P_m}{D_{nm}} - \rho_{nm} \; g_{nm} \right) \; , \tag{3}$$

where

A_{nm} the common area between gridblocks n and m $[L^2]$;

k intrinsic permeability $[L^2]$;

k_{rw} relative water permeability $[dimensionless]$;

μ_w water dynamic viscosity $[ML^{-1}T^{-1}]$;

P water pressure $[ML^{-1}T^{-2}]$;

D_{nm} distance between nodal points n and m $[M]$;

g_{nm} component of the gravitational acceleration in the direction of m to n $[LT^{-2}]$.

The subscript nm denotes appropriate averaging over the parameters of gridblocks V_n and V_m.

2.3. The Tracer Equations

2.3.1. Conservation Equation

The conservation of mass for any subdomain n is given by equation (1), which in space-discretized form assumes the form of the following ordinary differential equation:

$$\left(\frac{dM_i}{dt}\right)_n = \frac{1}{V_n}\sum_m A_{nm}(F_i)_{nm} + (q_i)_n, \tag{4}$$

where $(F_i)_{nm}$ is the mass flux of tracer i between elements n and m $[MLT^{-1}]$, and $(q_i)_n$ is the mass rate of the source/sink of tracer i in element n $[MT^{-1}]$.

2.3.2. Accumulation Terms

The accumulation term M of a tracer i in a porous or fractured medium (PFM) is given by

$$M_i = \begin{cases} M_{L,i} + M_{Ag,i} + \delta_{\mathcal{R}}\, M_{\mathcal{R},i} + \delta_c\, M_{Ac,i} & \text{for solutes} \\ M_{L,i} + M_{F,i} + \delta_{\mathcal{R}}\, M_{\mathcal{R},i} & \text{for colloids} \end{cases} \tag{5}$$

where

$M_{L,i}$ the mass of tracer i (solute or colloidal) in the the aqueous phase $[ML^{-3}]$;

$M_{Ag,i}$ the mass of solute tracer i adsorbed onto the PFM grains $[ML^{-3}]$;

$M_{\mathcal{R},i}$ the reacted mass of tracer i (solute or colloidal) in the the aqueous phase $[ML^{-3}]$;

$M_{Ac,i}$ the mass of solute tracer i adsorbed onto colloidal particles $[ML^{-3}]$;

$M_{F,i}$ the mass of filtered colloidal tracer i $[ML^{-3}]$.

and the parameters

$$\delta_R = \begin{cases} 1 & \text{for reactive solutes or reactive "real" colloids;} \\ 0 & \text{otherwise} \end{cases} \tag{6}$$

and

$$\delta_c = \begin{cases} 1 & \text{for "pseudocolloids"} \\ 0 & \text{otherwise.} \end{cases} \tag{7}$$

The term "real" colloids refers to those generated from contaminants [*Saltelli et al.*, 1984] when their concentrations exceed their solubility [*van der Lee et al.*, 1992], and their study focuses on their transport. Colloids from other sources (e.g., clay particles naturally ocurring in the subsurface) are termed "pseudocolloids" [*Ibaraki and Sudicky*, 1995], and their study includes both colloid transport and sorption of contaminants onto them. A detailed discussion on the subject can be found in *Ibaraki* [1994] and [*Ibaraki and Sudicky*, 1995]. EOS9nT allows the study of both types of colloids.

Omitting for simplicity the i subscript, M_L is obtained from

$$M_L = \phi\,(S_w - S_r)\,\rho\,X + \phi\,S_r\,\rho\,\mathcal{X}\,, \tag{8}$$

where

X the tracer mass fraction in the mobile fraction of the aqueous phase $[M/M]$;

$\mathcal{X}$ the tracer mass fraction in the immobile fraction of the aqueous phase $[M/M]$;

S_r the irreducible water saturation $[L^3/L^3]$.

Equation (8) reflects the fact that solute concentrations are different in the mobile and immobile water fractions, and incorporates the approximation that the immobile water saturation is the irreducible water saturation. Because water is very strongly bound (in electric double layers) to the PFM grain surface, Brownian motion is limited and solubility in the immobile water is lower than in the mobile water fraction. The importance of this boundary layer has been recognized by *de Marsily* [1986], who differentiates X and $\mathcal{X}$, and *Skagius and Neretnieks* [1986] and *Moridis* [1999], who use the mobile fraction of water in the analysis of diffusion experiments. Using the linear equilibrium relationship [*de Marsily*, 1986],

$$\mathcal{X} = K_t\,X, \tag{9}$$

where K_t is a dimensionless mass transfer coefficient (dimensionless). For solutes $1 \geq K_t > 0$. Because of their double layers and their relatively large size (compared

to solutes), colloids are expected to concentrate in the mobile water fraction and to be practically absent from the imobile water fraction. Then, a good approximation is $K_t \simeq 0$.

Substitution into (8) then leads to

$$M_L = \phi\, h\, \rho\, X, \quad \text{where} \quad h = S_w - S_r + K_t\, S_r\,. \tag{10}$$

2.3.3. *Sorption Terms*

Omitting again for simplicity the i subscript, the mass of a solute sorbed onto the PFM grains is given by

$$M_{Ag} = (1-\phi)\,\rho_s\, F\,, \tag{11}$$

where

ρ_s the rock density $[ML^{-3}]$;

F $= F_p + F_c$, the total sorbed mass of solute per unit mass of the PFM $[M/M]$;

F_p the physically sorbed mass of solute per unit mass of the PFM $[M/M]$;

F_c the chemically sorbed mass of solute per unit mass of the PFM $[M/M]$;

2.3.3.1. Equilibrium physical sorption. Following *de Marsily* [1986], and considering that sorption onto the soil grains occurs as the dissolved species diffuses through the immobile water fraction, the equilibrium physical sorption is described by the equation

$$F_p = \begin{cases} K_d\, \rho\, K_t\, X & \text{for linear equilibrium (LE) sorption,} \\ K_F\ (\rho\, K_t\, X)^{\beta} & \text{for Freundlich equilibrium (FE) sorption,} \\ \dfrac{K_1\, \rho\, K_t\, X}{1 + K_2\, \rho\, K_t\, X} & \text{for Langmuir equilibrium (LAE) sorption} \end{cases} \tag{12}$$

where K_d $[M^{-1}L^3]$, K_F $[M^{-\beta}L^{3\beta}]$, β, K_1 $[M^{-1}L^3]$, and K_2 $[M^{-1}L^3]$ are sorption parameters specific to each solute and rock type. Of particular interest is the parameter K_d, called the distribution coefficient, which is the constant slope of the linear equilibrium adsorption isotherm of a solute in relation to the medium.

2.3.3.2. Kinetic physical sorption. The kinetic sorption is given by

$$\frac{dF_p}{dt} = \begin{cases} k_\ell(K_d\,\rho\,K_t\,X - \delta_p\,F_p) & \text{for linear kinetic (LKP) sorption,} \\ k_F[K_F\,(\rho\,K_t\,X)^\beta - F_p] & \text{for Freundlich kinetic (FKP)sorption,} \\ k_L\left(\dfrac{K_1\,\rho\,K_t\,X}{1+K_2\,\rho\,K_t\,X} - F_p\right) & \text{for Langmuir kinetic (LAKP) sorption,} \end{cases} \tag{13}$$

where

$$\delta_p = \begin{cases} 1 & \text{for linear kinetic physical (LKP) sorption;} \\ 0 & \text{for linear irreversible physical (LIP) sorption,} \end{cases} \tag{14}$$

and k_ℓ, k_F and k_L are the kinetic constants for linear, Freundlich and Langmuir sorption, respectively $[T^{-1}]$. For $\delta_p = 0$, the linear kinetic equation in (13) can also be used to describe the chemical process of salt precipitation.

2.3.3.2. Kinetic chemical sorption. The first-order reversible chemical sorption is represented by the linear kinetic chemical (LKC) model

$$\frac{\partial F_c}{\partial t} = k_c^+\,\rho\,K_t\,X - k_c^-\,F_c\,, \tag{15}$$

where k_c^+ $[M^{-1}L^3T^{-1}]$ and k_c^- $[T^{-1}]$ are the forward and backward kinetic constants, respectively.

Note that in EOS9nT any two equations from (12), (13) or (15) can be used simultaneously to describe combined sorption [*Cameron and Klute*, 1977]. Combined sorption accounts for the different rates at which a species is sorbed onto different contituents of a single PFM. For example, sorption onto organic components may be instantaneous and follows a linear equilibrium isotherm. Sorption onto mineral surfaces may be much slower and follows a kinetic physical sorption isotherm, while ion exchange will follow a kinetic chemical sorption isotherm [*Cameron and Klute*, 1977].

2.3.4. Chemical Reaction Terms

Assuming that reactions occur only in the liquid phase, the mass of reacted tracer (solute or colloid) is given by

$$M_{\mathcal{R}} = \phi\, h\, \rho\, \mathcal{R}\,, \tag{16}$$

and $\mathcal{R}$ is obtained from the reaction kinetics. The kinetic equations of a chain of N_χ first-order chemical reactions are given by [*Cho*, 1971]

$$\begin{aligned}
\frac{\partial \mathcal{R}_1}{\partial t} &= \mathcal{K}_1\, \rho\, X_1\ , \\
\frac{\partial \mathcal{R}_2}{\partial t} &= \mathcal{K}_2\, \rho\, X_2 - \mathcal{K}_1\, \rho\, X_1\ , \\
&\vdots \qquad\qquad\qquad \vdots \\
\frac{\partial \mathcal{R}_{N_\chi}}{\partial t} &= \mathcal{K}_{N_\chi}\, \rho\, X_{N_\chi} - \mathcal{K}_{N_\chi - 1}\, \rho\, X_{N_\chi - 1}\ ,
\end{aligned} \tag{17}$$

where $\mathcal{K}_j$ $(j = 1, \ldots, N_\chi)$ is the chemical reaction rate constant $[T^{-1}]$, and N_χ is the number of chemical reactions in the chain. Implicit in (16) is the consideration of mass transfer through the immobile water fraction. Equations (16) and (17) apply to reactive solutes and reactive "true" colloids.

2.3.5. Colloid Filtration Terms

These are considered only when the tracer is a colloid. Colloidal particles moving through porous media are subject to filtration, the mechanisms of which have been the subject of several investigations, e.g., *Herzig et al.* [1970]; *Wnek et al.* [1975]; *Tien et al.* [1979]; *Corapcioglu et al.* [1987]. The mass of filtered colloids is then given by

$$M_{F,i} = \rho_{c,i}\, \sigma_i, \tag{18}$$

where $\rho_{c,i}$ is the density of the colloidal particles of colloid i $[ML^{-3}]$ and σ_i is the colloid concentration expressed as volume of colloids per volume of the porous medium $[L^3/L^3]$.

When colloid deposition is a relatively fast process compared to the groundwater velocity, it is possible to describe colloid filtration as a linear equilibrium process [*James and Chrysikopoulos*, 1999]. Omitting the i subscript, filtration is then described by

$$\sigma = K_\sigma \, K_t \, \rho \, X \,, \tag{19}$$

where K_σ is a distribution coefficient $[M^{-1}L^3]$.

The colloid filtration is generally non-equilibrium, and is more accurately described by a linear kinetic model [*Çorapçioglu et al.*, 1987], which can take the following form:

$$\frac{\partial \sigma}{\partial t} = \kappa \left(K_\sigma \, K_t \, C - \delta_p \, \sigma \right) = \kappa^+ C - \kappa^- \, \sigma \,, \tag{20}$$

where κ $[T^{-1}]$ is a kinetic coefficient, and κ^+ $[M^{-1}L^3T^{-1}]$ and κ^- $[T^{-1}]$ are the kinetic forward and reverse colloid deposition rates (clogging and declogging coefficients), respectively, which are specific to each colloid and medium. The parameter δ_p is analogous to that for sorption in equations (13) and 914), and describes the reversibility of filtration.

The term κ^- is commonly assumed to be zero [*Bowen and Epstein*, 1979], but there is insufficient evidence to support this. The parameter κ^+ can be given by

$$\kappa^+ = \kappa \, K_\sigma \, K_i \qquad \text{or} \qquad \kappa^+ = \epsilon \, f \, u \, G \,, \tag{21}$$

where ϵ is the filter coefficient of the porous medium $[L^{-1}]$, f is a dimensionless velocity modification factor, u is the Darcy velocity $[LT^{-1}]$, and G is a dimensionless dynamic blocking function (DBF) which describes the variation of the PFM porosity and specific surface with σ [*James and Chrysikopoulos*, 1999].

The first expression in (21) is similar to that for linear kinetic sorption, and is an approximation that can be used effectively in studies where the water flow velocities vary within a narrow range. An example of such an application would be the study of colloid filtration in 1-D systems (columns) under steady-state flow conditions, from which the κ^+

and κ^- parameters can be determined. The second expression in (21) is more general, applies to domains in which the flow velocity varies within a wide range [*de Marsily*, 1986], and is conceptually more robust because it considers the effects of flow velocity on colloid attachment.

There are several expressions describing the term ϵ. We compute ϵ according to *Harvey and Garabedian* [1991] as

$$\epsilon = 1.5 \frac{1-\phi}{d_m} \alpha_c \eta_c \,, \tag{22}$$

where d_m is the particle size of the medium grains or the fracture aperture $[L]$, and

$$\eta_c = 0.9 \left(\frac{k_B T}{\mu_w d_c d_m u} \right)^{2/3} + 1.5 \left(\frac{d_c}{d_m} \right)^2 + (\rho_c - \rho) \frac{g d_c^2}{18 \mu u} \tag{23}$$

in which k_B is the Boltzman constant, d_c is the colloid diameter $[L]$, α_c is the singe collector efficiency, T is the absolute temperature and all other terms remain as previously defined.

The factor f $(1 \leq f \leq 1.5)$ accounts for the fact that the velocity of the colloidal particle flow is larger than that of water. This is due to the relatively large size of the colloids, which tends to concentrate them in the middle of the pores where the groundwater velocity is larger. The f factor tends to increase with decreasing ionic strength [*Small*, 1974], but cannot exceed 1.5 because colloids cannot move faster that the maximum groundwater velocity [*Ibaraki and Sudicky*, 1995].

For deep filtration (i.e., in the case of very dilute colloidal suspensions), there is no interaction among the colloidal particles and no effects on the medium porosity and permeability, i.e., ϕ is constant, and $G = 1$. An analytical solution to this problem was developed by *Dieulin* [1982] by setting κ^- to zero. EOS9nT assumes deep filtration, thus preserving the linearity in the equations and the ability to decouple the flow and the transport equations.

2.3.6. Colloid-Assisted Transport Terms

The mass of a tracer i sorbed onto pseudocolloids is described by computed from

$$M_{Ac,i} = \sum_{j=1}^{N_c} (\rho_j \sigma_j + \rho X_j) \mathcal{F}_{i,j} \tag{24}$$

where $\mathcal{F}_{i,j}$ denotes the sorption of tracer i onto colloid j $[M/M]$, and N_c is the total number of pseudocolloids. The first term in the sum inside the parenthesis of equation (24) describes the filtered (deposited) colloid concentration, and the second the concentration of the suspended colloids in the liquid phase. $\mathcal{F}_{i,j}$ is computed from equations (12), (13) or (15), with the appropriate sorption parameters corresponding to each colloid. Note that equation (24) applies to pseudocolloids only, as opposed to true colloids, onto which radionuclides are not considered to sorb.

2.3.7. Flux Terms

2.3.7.1. General equations. The flux term has contributions from advective, diffusive and dispersive transport processes, and is given by

$$\mathbf{F}_i = \mathbf{F}_w \; X_i - \rho \; \mathbf{D}_i \; \nabla X_i - \mathbf{F}_{s,i} \; , \tag{25}$$

where $\mathbf{F}_{s,i}$ is the flux due to surface diffusion, and $\mathbf{D}_i$ is the dispersion tensor of tracer i, a second order symmetric tensor with a principal axis aligned with the Darcy flow vector and the other normal to it. Omitting the i subscript, $\mathbf{D}$ is described by the equations [*Moridis*, 1999]

$$\mathbf{D} = D^T \; \mathbf{I} + \frac{D^L - D^T}{u^2} \; \mathbf{u} \; \mathbf{u} \; , \tag{26}$$

$$D^L = \phi \, (S_w - S_r) \, \tau \, D_0 + \phi \, S_r \, \tau \, d + \alpha_L \, u \; , \tag{27}$$

$$D^T = \phi \, (S_w - S_r) \, \tau \, D_0 + \phi \, S_r \, \tau \, d + \alpha_T \, u \; , \tag{28}$$

where

$\mathbf{I}$ the unit vector ;

τ the tortuosity factor of the pore paths $[L^0]$;

D_0 the molecular diffusion coefficient of tracer i in water $[L^2T^{-1}]$;

α_L, α_T longitudinal and transverse dispersivities, respectively $[L]$;

$\mathbf{u}$ the Darcy velocity vector $[LT^{-1}]$.

Equation (25) accounts for surface diffusion, which can be responsible for significant transport in strongly sorbing media [*Jensen and Radke*, 1988; *Moridis*,1999]. The surface diffusion Flux is given by [*Jahnke*, 1986; *Jahnke and Radke*, 1987]

$$\mathbf{F}_s = (1-\phi)\,\rho_s\,\tau_s\,D_s \nabla F_p, \tag{29}$$

where τ_s is the tortuosity factor of the surface path $[L^0]$, D_s is the surface diffusion coefficient $[L^2T^{-1}]$, and F_p is the physical diffusion computed from equations (12) or (13). There is theoretical justification for the relationship $\tau_s = \frac{2}{3}\,\tau$[*Cook*, 1989].

2.3.7.2. The dispersion tensor. In the treatment of the general 3-D dispersion tensor, EOS9nT follows closely the approach of the radionuclide transport module T2R3D [*Wu et al.*,1996; *Wu and Mishra*, 1998] for TOUGH2. Velocities are averaged by using the *projected area weighting method*, in which a velocity component u_j $(j \equiv x, y, z)$ of the vector $\mathbf{u}$ is determined by vectorial summation of the components of all local connection vectors in the same direction, weighted by the projected area in that direction. This approach allows the solution of the transport problem in irregularly-shaped grids, in which the velocities normal to the interface areas are not aligned with the principal axes.

2.3.7.3. Application to colloid transport. Equations (25) through (29) apply to solutes, but need the following modifications to render them suitable to colloidal transport:

1. $\mathbf{F}_s = 0$ because surface diffusion does not occur in colloids.
2. The flux $\mathbf{F}_s$ and the Darcy velocities u are multiplied by the factor f (see section 2.3.5).

3. The dispersivities α_L and α_T are generally different from those for solutes [*Ibaraki*, 1994], and may be a function of the colloidal particle size.
4. The term d_0 is the colloidal diffusion coefficient in water $[L^2T^{-1}]$, and is described by the Stokes-Einstein equation as [*Bird et al.*, 1960]

$$D_0 = \frac{k\,T}{3\,\pi\,\mu_w\,d_c}\,, \tag{30}$$

where k is the Boltzmann constant ($1.38 \times 10^{-23}\ J\,K^{-1}$ in SI units), T is the absolute water temperature $[K]$, μ_w is the dynamic viscosity of water $[MLT^{-1}]$. *Hiemenz* [1986] reported colloid D_0 values in the 10^{-11} m^2s^{-1} range.

5. The fluxes in equation (25) are multiplied by the colloid accessibility factors f_c $(0 \geq f_c \leq 1)$ at the interface of different media. The f_c factor describes the portion of the colloidal concentration in a medium that is allowed to enter an adjacent medium of different characteristics, and quantifies pore size exclusion (straining).

2.3.8. Radioactive Decay

When a tracer i undergoes radioactive decay, the rate of mass change is described by the first-order decay law

$$\frac{dM_i}{dt} = -\lambda_i\,M_i\ , \quad \text{where} \quad \lambda_i = \frac{\ln 2}{(T_{1/2})_i}\ , \tag{31}$$

and $(T_{1/2})_i$ is the half life of tracer i. Substitution of equations (15) and (19) into equation (4) yields

$$\left(\frac{dM_i}{dt}\right)_n + \lambda_i\,(M_i)_n = \frac{1}{V_n}\sum_m A_{nm}\,[F_{nm}\,X_i - \rho\ \mathbf{D}_i\ \nabla X_i - \mathbf{F}_{s,i}] + (q_i)_n \tag{32}$$

2.3.9. Daughter Products of Radioactive Decay or Reaction Chain

If a radioactive tracer i is a daughter product of the decay of tracer j, then the rate of mass change is described by [*de Marsily*, 1986; *Oldenburg and Pruess*, 1995] as

$$\left(\frac{dM_i}{dt}\right)_n + \lambda_i \left(M_i\right)_n - \lambda_{i-1}\, m_r \left(M_{i-1}\right)_n = \frac{1}{V_n} \sum_m A_{nm} \left[F_{nm}\, X_i - \rho\ \mathbf{D}_i\ \nabla X_i - \mathbf{F}_{s,i}\right] + \left(q_i\right)_n , \tag{33}$$

where $m_r = W_i/W_{i-1}$, and W_i and W_{i-1} are the molecular weights of the daughter and parent species, respectively. Equation (33) applies to radioactive solutes or radioactive true colloids. By saving the M_i terms, EOS9nT is capable of tracking any number of daughters.

For daughters following an isotherm other than LE, equations (13) and (15) need to account for the generation of daughter mass from the decay of the sorbed parent, and become

$$\frac{\partial F_i}{\partial t} + \lambda_\kappa\, F_\nu - \lambda_{i-1}\, m_r\, \zeta_i\, F_{i-1} = k_A\, C_i\ - k_B \left(F_i + m_r\, \zeta_i F_{i-1}\right) , \tag{34}$$

where F_{i-1} is the sorbed mass of the parent,

$$k_A = \begin{cases} k_\ell\, K_d\, K_i & \text{for LKP/LIP sorption,} \\ k_c^+\, K_i & \text{for LKC sorption,} \end{cases} \qquad k_B = \begin{cases} k_p\, \delta_p & \text{for LKP/LIP sorption,} \\ k_c^- & \text{for LKC sorption,} \end{cases}$$

and ζ_i is the fraction of the mass of the decayed sorbed parent that remains sorbed as a daughter ($0 \le \zeta_i \le 1$). The term ζ_i is introduced to account for the different sorption behavior of parents and daughters, and the fact that daughters can be ejected from grain surfaces due to recoil (e.g., the ejection of ^{234}Th from grain surfaces during the alpha decay of ^{238}U) [*Faure*, 1977].

For daughter products of reactive chains, the rate of mass change is given by

$$\left(\frac{dM_i^-}{dt}\right)_n + \left(\phi\, h\, \mathcal{K}_i\, \rho\, X_i\right)_n - \left(\phi\, h\, \mathcal{K}_{i-1}\, \rho\, X_{i-1}\right)_n = \frac{1}{V_n} \sum_m A_{nm} \left[F_{nm}\, X_i - \rho\ \mathbf{D}_i\ \nabla X_i - \mathbf{F}_{s,i}\right] + \left(q_i\right)_n , \tag{35}$$

where $M_i^- = M_i - M_{\mathcal{R},i}$. By saving the X_i values of the chain members, EOS9nT is capable of tracking any number of daughter products of the reaction chain.

2.3.10. An important Issue

It is important to know that EOS9nT allows the study of either a radioactive decay chain or a reactive chain, but not both. An attempt to consider both causes EOS9nT to print an error message and abort the simulation.

3. Time Discretization and Matrix Solution

3.1. Conventional Timestepping

Using the conventional timestepping approach of TOUGH2 [*Pruess*, 1991], time in EOS9nT is discretized using a first-order finite difference approximation. The treatment of the flux and sink/source terms is *fully implicit*, i.e., they are evaluated at the new time level to obtain the numerical stability needed for an efficient calculation of flow and transport. The residuals are determined, and the elements of the Jacobian matrix are computed following the approach described in detail by *Pruess* [1987;1991]. The Jacobian is then solved using a set of preconditioned conjugate gradient solvers available in TOUGH2 [*Moridis and Pruess*, 1995;1998]. The matrix development and solution have been the subject of detailed descriptions in the aforementioned reports, and will not be further discussed here.

The evolution of the timestep size in the flow component of EOS9nT follows the conventional TOUGH2 approach, and is internally controlled by the Newtonian convergence criteria [*Pruess*, 1991]. The timestep size in the n transport equations is specific to each

tracer, and is controlled by inputs which place limitations on its magnitude based on (a) the user-defined maximum allowed grid Courant number and (b) the maximum allowable fraction of the SC half-life $(T_{1/2})_i$ (if radioactive). It must be pointed out that the fully implicit formulation of EOS9nT with upstream weighting does not place any limitations on the Courant number. This is a consideration only in explicit schemes. A user-defined maximum allowed Courant number in EOS9nT is a means of setting an upper boundary to the timestep magnitude in the transport equations.

Under transient flow conditions, the time-stepping process in EOS9nT is shown in Figure 1, in which Δt_f is the timestep in the flow equation and $\Delta t_{t,i}$ is the timestep in the transport equation of tracer i. A total of $n+1$ separate simulation times are independently tracked in EOS9nT.

After the flow solution at $t + \Delta t_f$ is obtained, the water saturations, flow velocities and flow rates across the element interfaces are recorded. The time is then reset to t in the transport equation of tracer i, and the maximum allowable $\Delta t_{t,i}$ is determined from limitations on the grid Courant number and the tracer half life. The tracer transport in the Δt_f interval is simulated using a total of $k_i \leq \Delta t_f / \Delta t_{t,i}$ generally unequal time steps, where k_i is the next largest integer of the $\Delta t_f / \Delta t_{t,i}$ ratio. The $\Delta t_{t,i}$ within any given Δt_f are generally unequal because their size increases if the Jacobian converges within a preset number of Newtonian iterations, in a manner identical to the timestep size in the flow component [*Pruess*, 1991]. The process is repeated for all n independently-tracked tracers. The time step sizes of the various tracers are not generally equal.

If the tracer is a colloid whose filtration is considered to have an effect on flow, the saturation of filtered colloids is computed from equation (22). At the end of the solution of the transport equations, i.e., at $t + \Delta t_f$, the saturations are adjusted using equations (22) and (23). For the next flow timestep, the adjusted saturations are used to compute the water relative permeability and the capillary pressure.

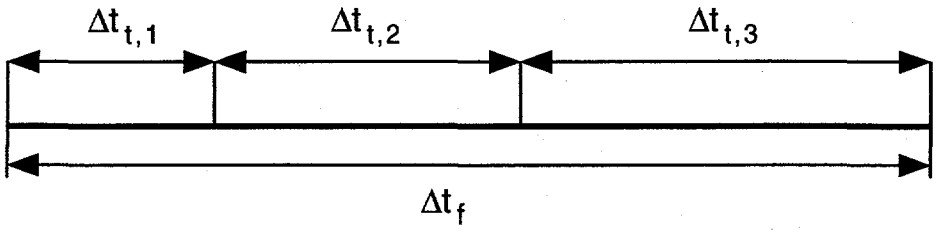

Figure 1. Timestepping in EOS9nT.

As the flow field becomes invariant, the size of the Δt_f in TOUGH2 increases, and convergence is achieved after a single Newtonian iteration. Contrary to the standard TOUGH2, which prints the invariant solution and stops the simulation after 10 such time steps of convergence on the first iteration, EOS9nT prints the flow solution and continues solving the tracer equations. The time step in the solute transport equations becomes uniform and equal to the shortest of the $\Delta t_{t,i}$ $(i = 1, \ldots, n)$ after the flow has reached a steady state.

EOS9nT also allows tracer transport simulations when the initial flow field is time-invariant. In this case, EOS9nT solves the flow field only once in order to obtain the constant water saturations, flow velocities and flow rates across the element interfaces. After printing the flow data, only the tracer transport equations are solved.

The Courant number limitations may result in a situation where the smallest gridblock controls the $\Delta t_{t,i}$, and may result in inefficient simulations and excessive computational times. To partially alleviate this problem, EOS9nT determines the $\Delta t_{t,i}$ from limitation on the Courant numbers at gridblocks at which the changes in X_i are within 5% of the maximum change. This allows timestep adjustment by tracking a moving front, and limits Courant number considerations to elements where measurable changes occur.

3.2. Laplace Transform Formulation

In problems in which the flow field is invariant and solutions are required at very large times, the Courant and half-life limitations in conventional timestepping may result $\Delta t_{t,i}$ which are too short for an efficient simulation, thus requiring impractically long execution times. To address this problem, EOS9nT offers an optional Laplace transform formulation for the solution of the transport problem in time-invariant flow fields.

The major advantage of this formulation is that it eliminates the need for time discretization, and avoids the problems stemming from the treatment of the time derivatives in the transport equations. It yields solutions semi-analytical in time and numerical in space by solving special formulations of the PDEs using the integral finite difference space discretization scheme of TOUGH2 [*Pruess*, 1991] in the Laplace space, and numerically inverting the transformed solution vectors. Concerns over the effects of the numerical treatment of the time dependency on accuracy and stability, which necessitate a large number of small time steps between successive observation times in conventional timestepping solutions, are rendered irrelevant because time is no longer a consideration. An unlimited time step size is thus possible without loss of accuracy or stability.

As application of the Laplace space formulation demands strict linearity of (or ability to linearize the) problem. Thus, the Laplace formulation in EOS9nT may not be used under the following conditions:

1. The flow is transient.
2. The physical sorption does not follow a linear equilibrium or linear kinetic isotherm.
3. Colloid-assisted transport is considered.
4. The porosity and permeability of the medium are affected by the colloid filtration.

3.2.1. *The Laplace Space Transport Equations*

In its most general form, the Laplace transform of the derivative of the accumulation terms of a daughter product i from the decay of parent $i-1$ in equation (33) yields

$$\begin{aligned}\mathcal{L}\{\frac{dM_i}{dt} + \lambda_i M_i - \lambda_{i-1} m_r M_{i-1}\} \\ = \left[\phi h \rho \widehat{X}_i + (1-\phi)\rho_s \widehat{F}_i\right](s+\lambda_i) - \lambda_{i-1} m_r \widehat{M}_{i-1} \\ - \left[\phi h \rho X_{i,0} + (1-\phi)\rho_s F_{i,0}\right],\end{aligned} \tag{36}$$

where s is the Laplace space parameter, $\hat{\alpha} = \mathcal{L}\{\alpha\}$, $\mathcal{L}\{\}$ denotes the Laplace transform of the term within the brackets, and the subscript 0 of X_i and F_i denotes their values at $t = 0$. For a stable isotope, $\lambda_i = 0$. For a parent, the term $\lambda_{i-1} m_r \widehat{M}_{i-1} = 0$.

Similarly, the Laplace transform of the derivative of the accumulation terms of a daughter product i from the reaction of parent $i-1$ in equation (35) yields

$$\begin{aligned}\mathcal{L}\left\{\frac{dM_i^-}{dt} + \phi h \rho(\mathcal{K}_i X_i - \mathcal{K}_{i-1} X_{i-1})\right\} \\ = \phi h \rho (s + \mathcal{K}_i)\widehat{X}_i + (1-\phi)\rho_s s \widehat{F}_i - \phi h \rho \mathcal{K}_{i-1} \widehat{X}_{i-1} \\ - \left[\phi h \rho X_{i,0} + (1-\phi)\rho_s F_{i,0}\right].\end{aligned} \tag{37}$$

From *Moridis and Bodvarsson* [1999],

$$\widehat{F} = \gamma \widehat{X} + \theta, \tag{38}$$

where

$$\gamma = \begin{cases} w & \text{for LE sorption,} \\ u & \text{for LKP or LIP sorption,} \\ v & \text{for LKC sorption,} \\ w+u & \text{for combined LE and LKP/LIP sorption,} \\ w+v & \text{for combined LE and LKC sorption,} \\ u+v & \text{for combined LKP/LIP and LKC sorption,} \end{cases} \tag{39}$$

$$\theta = \begin{cases} 0 & \text{for LE sorption,} \\ u_1 & \text{for LKP or LIP sorption,} \\ v_1 & \text{for LKC sorption,} \\ u_1 & \text{for combined LE and LKP/LIP sorption,} \\ v_1 & \text{for combined LE and LKC sorption,} \\ u_1 + v_1 & \text{for combined LKP/LIP and LKC sorption,} \end{cases} \tag{40}$$

$$w = K_d\, K_t\, \rho, \qquad u = \frac{k_p\, K_d\, K_t\, \rho}{s + \lambda + \delta_p\, k_p}, \qquad v = \frac{k_c^+\, K_t\, \rho}{s + \lambda + k_c^-}, \tag{41}$$

and

$$u_1 = \frac{F_{p,0}}{s + \lambda + \delta_p\, k_p}, \qquad v = \frac{F_{c,0}}{s + \lambda + k_c^-}, \tag{42}$$

where the 0 subscript of F_p and F_c denotes their values at $t = 0$. For non-radioactive substances, $\lambda = 0$, and equations (36) through (42) apply unchanged.

For colloids, the term $(1 - \phi)\, \rho_s\, \widehat{F}$ in equation (36) and (37) is replaced by $\rho_c\, \widehat{\sigma}$, where

$$\widehat{\sigma} = \overbrace{\frac{\kappa^+\, K_\sigma\, \rho}{s + \kappa^- + \lambda)}}^{\gamma}\ \widehat{X}\ + \overbrace{\frac{\sigma_0}{s + \kappa^- + \lambda}}^{\theta}\ . \tag{43}$$

Thus, equation (38) applies after substituting σ for F. Similarly, the term $(1 - \phi)\, \rho_s\, F_0$ in equation (36) and (37) is replaced by $\rho_c\, \sigma_0$, where the 0 subscript denotes the value at $t = 0$. This formulation allows simulation of radioactive true colloids. For pseudocolloids, $\lambda = 0$ in equation (43).

Taking the Laplace transform of equation (33) results (after the appropriate substitutions) in the form

$$\mathcal{M}_i\, \widehat{X}_i - \frac{1}{V_n} \sum_m A_{nm} \left[F_{nm}\, \widehat{X}_i - \mathbf{D}_i^*\ \nabla \widehat{X}_i \right] = \mathcal{H}_i - \lambda_{i-1}\, m_r\, \widehat{M}_{i-1}, \tag{44}$$

where

$$\mathcal{M}_i = \begin{cases} \phi\, h\, \rho(s + \mathcal{K}_i) + (1 - \phi)\, \rho_s\, \gamma_i\, s & \text{in reactive chains} \\ [\phi\, h\, \rho + (1 - \phi)\, \rho_s\, \gamma_i]\, (s + \lambda_i) & \text{otherwise} \end{cases} \tag{45}$$

$$\mathbf{D}_i^* = \rho\ \mathbf{D}_i + (1-\phi)\,\rho_s\,\tau_s\,D_s\,\gamma_i\,, \tag{46}$$

$$\mathcal{H}_i = -\left\{\phi\,h\,\rho\,X_{i,0} + (1-\phi)\,\rho_s\,\left[1-\theta_i\,(s+\lambda_i)\right]\,F_{i,0} + \widehat{Q}_i\right\}\,, \tag{47}$$

$$\widehat{Q}_i = \mathcal{L}\{q_i\} = \begin{cases} q_w\,X_{qi}/s & \text{for a source,} \\ q_w\,(\widehat{X}_i)_n & \text{for a sink,} \end{cases} \tag{48}$$

q_w is the water mass injection or withdrawal rate, and $X_{q,i}$ is the mass fraction of tracer i in the injected stream. In EOS9nT the terms $\widehat{M}_j$ are saved from the simulation of the parent, and are subsequently used in the computation of the distribution of any parent.

Equations (44) through (48) apply to both solute and colloid transport by employing the appropriate γ and θ values, i.e., equations (39) through (42) for solutes, or equation (43) for colloids. It is obvious that for a non-radioactive, non-reactive tracer, either of the two expressions in (45) return the same $\mathcal{M}_i$. An important point is that γ_i in (46) reflects physical sorption only, and consequently its computation does not involve any v terms in equation (39). Finally, application of equation (47) to reactive chains implies setting $\lambda_i = 0$, as EOS9nT does not accommodate concurrent radioactive and chemically reactive species.

3.2.2. The Laplace Space Solutions

Equation (44) is the Laplace space equation of transport. The resulting algebraic equations may be written in a general matrix form as:

$$\mathbf{T}\ \vec{\widehat{X}} = \vec{B}\ , \tag{49}$$

where $\mathbf{T}$ is the coefficient matrix, $\vec{\widehat{X}}$ is the vector of the unknowns, and $\vec{B}$ is the composite vector of knowns. Additional information on the implementation of the Laplace space formulation can be found in *Moridis* [1998].

The computation of $\mathbf{T}$ and $\vec{B}$ necessitates values for the s parameter of the Laplace space. These are provided by two numerical inversion schemes: the Stehfest algorithm [*Stehfest*, 1970*a*] and the *De Hoog et al.* [1982] method.

3.2.3. *The Stehfest Algorithm*

For a desired observation time t, the s in the Stehfest algorithm [*Stehfest*, 1970*a*; 1970*b*] is real and given by

$$s_\nu = \frac{\ln 2}{t} \cdot \nu, \qquad \nu = 1, \ldots, N_S \tag{50}$$

where N_S is the number of summation terms in the algorithm and is an even number.

The unknown vector $\vec{X}$ at any time t is obtained by by numerically inverting the Laplace space solutions $\vec{\hat{X}}(s_\nu)$ according to the equation

$$\vec{X}(t) = \frac{\ln 2}{t} \sum_{\nu=1}^{N_S} W_\nu \, \vec{\hat{X}}(s_\nu) \ , \tag{51}$$

where

$$W_\nu = (-1)^{\frac{N_S}{2}+\nu} \sum_{k=\frac{1}{2}(\nu+1)}^{\min\{\nu, \frac{N_S}{2}\}} \frac{k^{\frac{N_S}{2}}(2k!)}{(\frac{N_S}{2}-k)!k!(k-1)!(\nu-k)!(2k-\nu)!} \ . \tag{52}$$

Although the accuracy of the method is theoretically expected to improve with increasing N_S, *Stehfest* [1970*a*;1970*b*] showed that with increasing N_S the number of correct significant figures inreases linearly at first and then, due to roundoff errors, decreases linearly. He determined that the optimum N_S was 10 for single-precision variables (8 significant figures) and 18 for double-precision variables (16 significant figures). *Moridis and Reddell* [1991] reported that the method seems to be insensitive to N_S for $6 \leq N_S \leq 20$ in the solution of the equation of flow through porous media.

3.2.4. *The De Hoog Method*

In the method of *De Hoog et al.* [1982], hereafter referred to as the De Hoog method, s is a complex number given by *Crump* [1976] as

$$s_\nu = s_0 + \frac{\nu\pi}{T} \, j, \qquad s_0 = \mu - \frac{\ln(E_R)}{2T}, \qquad \nu = 1, \ldots, N_H \tag{53}$$

where $2T$ is the period of the Fourier series approximating the inverse function in the interval $[0, 2T]$, $j = \sqrt{-1}$, and $N_H = 2M_H + 1$ is an odd number. *Moridis* [1992] showed that very accurate solutions were obtained when $\mu = 0$, $10^{-12} \leq E_R \leq 10^{-9}$, and $0.9\, t_{max} \leq T \leq 1.1\, t_{max}$, where t_{max} is the maximum simulation time.

The inversion of the Laplace space solution obtained with the De Hoog method is far more complicated than in the Stehfest algorithm. The solution $\vec{X}(t)$ is given by

$$\vec{X}(t) = \frac{1}{T} \exp(s_0 t)\, \mathrm{Re}\left[\frac{A_{2M_H}}{B_{2M_H}}\right], \tag{54}$$

where

$$A_n = A_{n-1} + d_n\ z\ A_{n-2}, \quad B_n = B_{n-1} + d_n\ z\ B_{n-2}, \quad n = 1, \ldots, 2M_H, \tag{55}$$

$$z = \exp\left(\frac{j\,\pi\,t}{T}\right), \tag{56}$$

$$A_{-1} = 0, \quad A_0 = d_0, \quad B_{-1} = B_0 = 1\,, \tag{57}$$

$$d_0 = a_0, \quad d_{2m-1} = -q_m^{(0)}, \quad d_{2m} = -e_m^{(0)}, \qquad m = 1, \ldots, M_H, \tag{58}$$

$$\begin{aligned} &\text{for } \ell = 1, \ldots, M_H, \quad e_\ell^{(k)} = q_\ell^{(k+1)} - q_\ell^{(k)} + e_{\ell-1}^{(k+1)}, \quad k = 0, \ldots, 2M_H - 2\ell\,, \\ &\text{for } \ell = 2, \ldots, M_H, \quad q_\ell^{(k)} = q_{\ell-1}^{(k+1)}\ e_{\ell-1}^{(k+1)} / e_{\ell-1}^{(k)}, \quad k = 0, \ldots, 2M_H - 2\ell - 1, \end{aligned} \tag{59}$$

$$e_0^{(k)} = 0 \text{ for } k = 0, \ldots, 2M_H \quad \text{and} \quad q_1^{(k)} = a_{k+1}/a_k \text{ for } k = 0, \ldots, 2M_H - 1, \tag{60}$$

and

$$a_0 = \frac{1}{2} X(s_0), \qquad a_k = X(s_k). \tag{61}$$

A convergence acceleration is obtained if, on the last evaluation of the recurrence relations, $d_{2M_H}\ z$ in (53) is replaced by $R_{2M_H}(z)$,

$$R_{2M_H}(z) = -h_{2M_H}\left[1 - \sqrt{(1 + d_{2M_H}\ z/h_{2M_H})}\right], \tag{62}$$

where

$$h_{2M_H} = \frac{1}{2}[1 + z\ (d_{2M_H-1} - d_{2M_H})], \tag{63}$$

giving

$$\widehat{A}_{2M_H} = A_{2M_H-1} + R_{2M_H}\ A_{2M_H-2}, \qquad \widehat{B}_{2M_H} = B_{2M_H-1} + R_{2M_H}\ B_{2M_H-2}, \tag{64}$$

in which case the accelerated solution at a time t is given by replacing A_{2M_H} and B_{2M_H} by $\widehat{A}_{2M_H}$ and $\widehat{B}_{2M_H}$, respectively, in (54).

All the operations in equations (53) through (64) involve complex variables. *Moridis* [1992] determined that the minimum M_H for an acceptable accuracy is 5 ($N_H = 11$), and that for an accuracy comparable to that of the Stehfest method $M_H \geq 6$ ($N_H \geq 13$). The unique advantages of the De Hoog formulation is that (a) it is capable of accurately inverting very steep solution surfaces, and (b) a whole range of solutions at times t in the range $[0, T]$ can be obtained from a single set of Laplace space solutions, i.e., equation (49) needs not be solved for each t of interest.

3.2.5. Computational Issues

The order of the matrix equation in the EOS9nT simulations depends on the treatment of time. For conventional timestepping or the Stehfest Laplace formulation, the matrix is of order N, where N is the number of gridblocks in the domain. For the De Hoog formulation of the Laplace space solution, the matrix is still or order N, but is complex. To avoid using the rather slow complex arithmetic, the order of the matrix is increased to $2N$ by separating the real and the imaginary parts. An efficient set of Preconditioned Conjugate Gradient (PCG) methods is used to solve the equations. Details on the PCG methods and their preconditioning can be found in *Moridis and Pruess* [1995;1998].

4. Design and Implementation of EOS9nT

4.1. EOS9nT Structure and Design

The name of the EOS9nT module file (written in the FORTRAN77 language of TOUGH2) is `EOS9nT.f`, and includes the following subroutines:

(1) `INPUT(*)`
(2) `RFILE(*)`
(3) `EOS`
(4) `FINDS`
(5) `OUT(*)`
(6) `MULTI`
(7) `RAND`
(8) `TOUT`
(9) `WRISAV`
(10) `CYCIT(*)`
(11) `LINEQ(*)`
(12) `RELP(*)`
(13) `PCAP(*)`
(14) `ELINDX`
(15) `SORT`
(16) `UNITV`

(17) DTNSOR
(18) VELWTM
(19) GRADX
(20) BALLA (*)
(21) COURNT
(22) TCYCIT
(23) QTRACR
(24) TMULTI
(25) COLSOR
(26) LCYCIT
(27) LQTRCR
(28) LMULTI
(29) LGRADX
(30) LPACON
(31) HCYCIT
(32) HQTRCR
(33) HMULTI
(34) HTOUT
(35) HPACON

Running TOUGH2 with the EOS9nT module involves compilation and linking of the following modules and in the following order:

(1) T2CG1.f
(2) EOS9nT.f
(3) T2F.f
(4) MESHM.f
(5) MA28.f
(5) TRCOMN.f

The module TRCOMN.f provides array and COMMON declarations and dimensions. Some compilers may require renaming duplicate subroutine names (identified by an asterisk next to their name in the above list). Note that it is necessary to rename the LINEQ subroutine in T2CG1.f, as failure to do so would create problems because of changes in the argument list of the subroutine.

4.2. Additional EOS9nT Capabilities

In addition to the processes discussed in Section 2.1., EOS9nT, as a member of the TOUGH2 family of codes, shares all the general attributes of the family. Thus, it can handle multi-dimensional flow domains and cartesian, cylindrical or irregular grids. It can also handle matrix-fracture interactions for flow through fractured rocks. These capabilities are identical to those in the T2R3D module, and a full description can be found in *Wu et al.* [1998].

In EOS9nT initialization is possible using (a) pressure (b) water saturation or (c) capillary pressure. Additionally, EOS9nT has the capability of determining the initial pressure and/or water saturation distribution (gravity-capillary equilibrium) in relation to an initial, areally variable watertable elevation map provided during input.

EOS9nT has integrated capabilities to describe statistical heterogeneity (see Section 5.1). This is accomplished by using domain permeability modifiers, which can be externally supplied or internally generated using linear or logarithmic modifications based on random numbers. Scaling of the capillary pressures is then obtained by using the *Leverett* [1941] function.

4.3. Information Flow in EOS9nT

The flow of information in EOS9nT is depicted by the simplified flowchart of Figure 2, which shows some of the most important computation stages and subroutines.

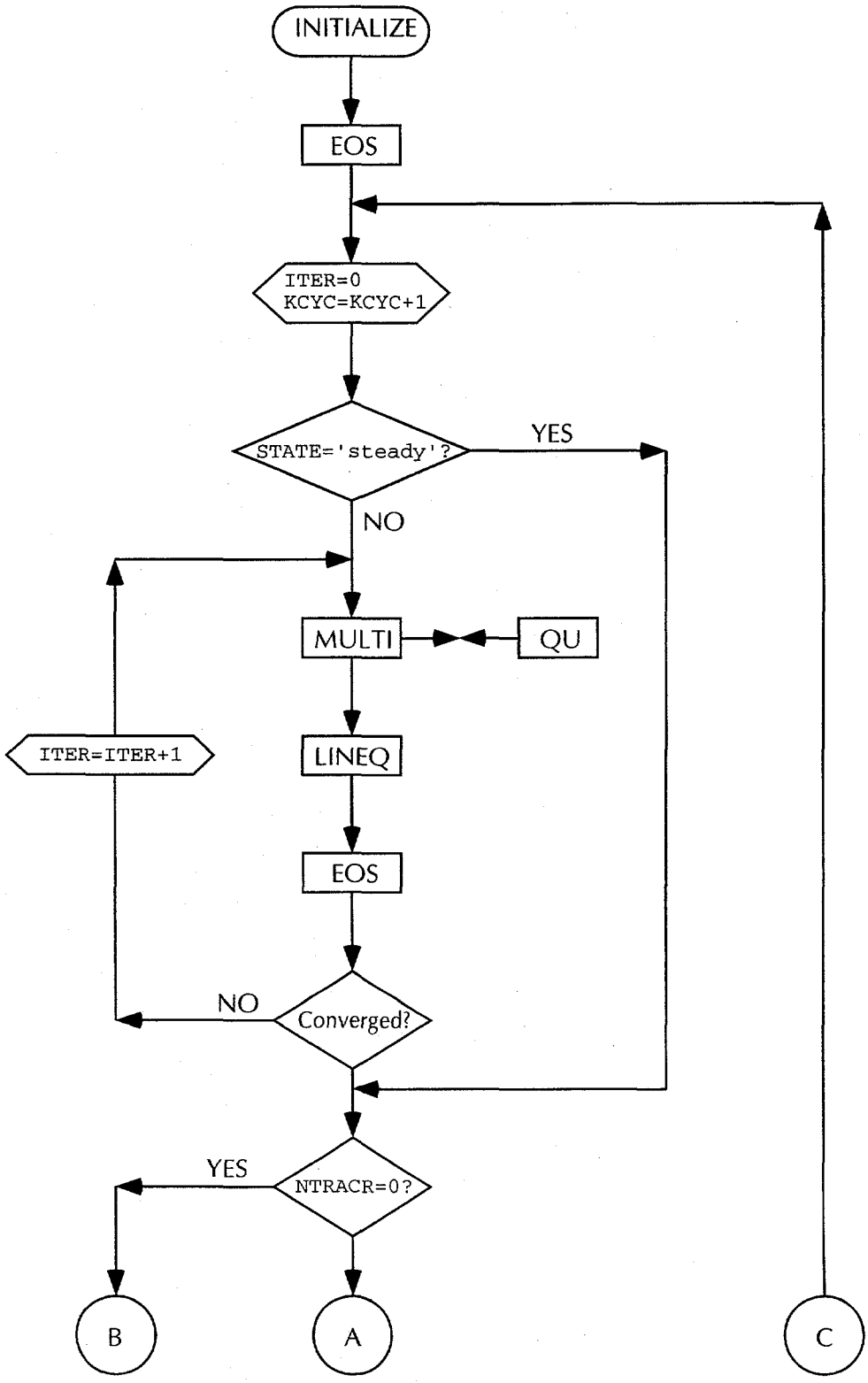
INITIALIZE
EOS
ITER=0
KCYC=KCYC+1
STATE='steady'?
YES
NO
MULTI
QU
ITER=ITER+1
LINEQ
EOS
NO
Converged?
YES
NTRACR=0?
B
A
C

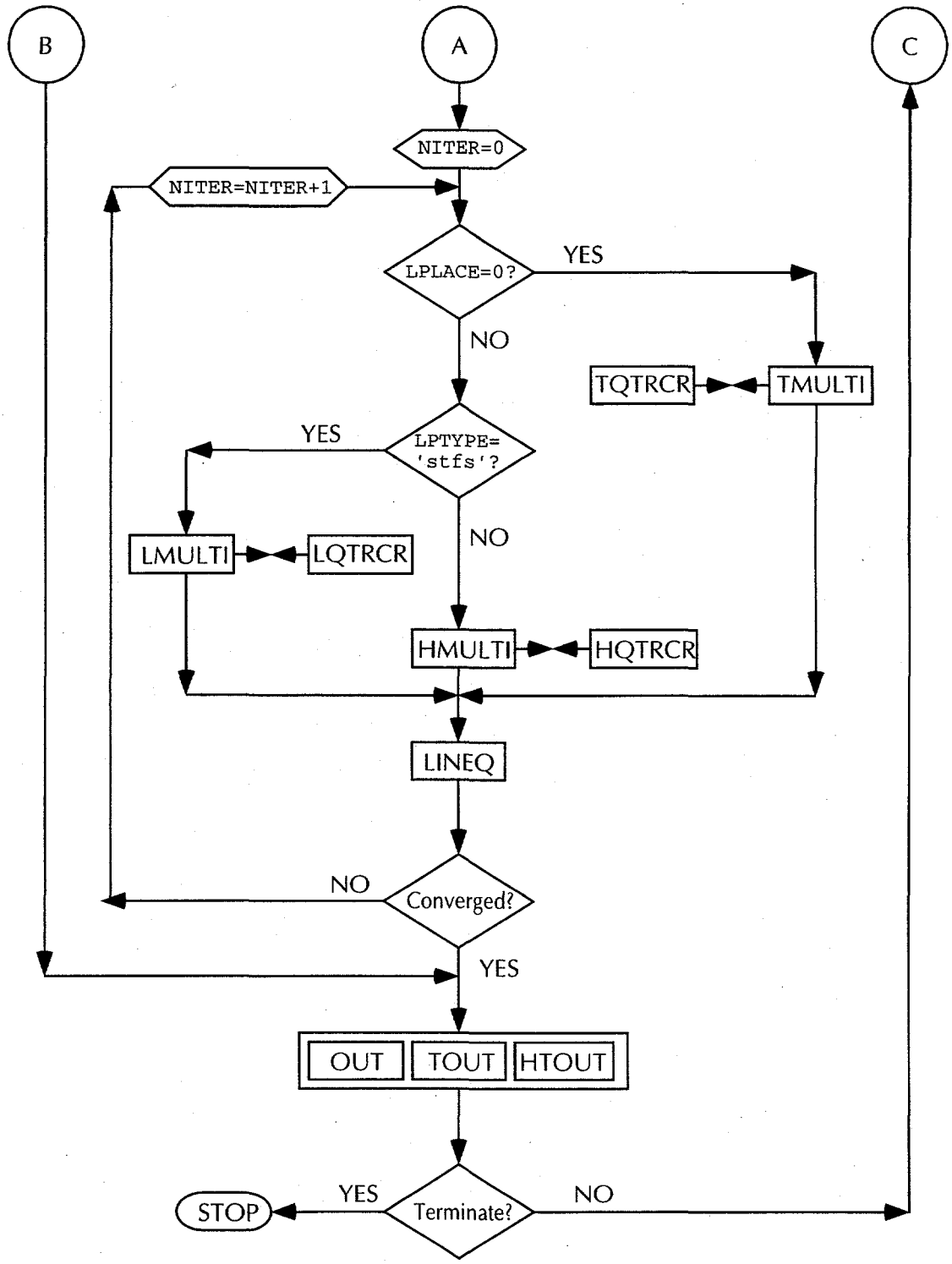

Figure 2. A simlified flowchart of EOS9nT .

5. Input Data Requirements and Specifications

5.1. Data Block ROCKS

5.1.1. Card ROCKS.1

If the parameter POR (i.e., the rock porosity) $\geq$ 2, EOS9nT automatically sets ALPHAL=ALPHAT=0.0 (i.e., $a_L = a_T = 0$ in equations (16) and (17)) in ROCKS.1.1 (see Section 5.1.2). Moreover, it resets the tortuosity TORT=0.0 in card ROCKS.1.1. This allows the use of *atmospheric* gridblocks and alleviates the non-physical behavior of tracers diffusing into these gridblocks.

5.1.2. Card ROCKS.1.1

Card ROCKS.1.1 reads the following:

```
COM,EXPAN,CDRY,TORT,GK,ALPHAL,ALPHAT,TRANCO,PHIF
```

according to the format

```
FORMAT(7E10.4,F4.2,F6.4)
```

The parameters COM, EXPAN, CDRY, TORT remain as previously described in TOUGH2 [*Pruess*, 1987;1991]. The other parameters are as follows.

GK	The immobile water saturation S_r – see equation (8).
ALPHAL	The solute longitudinal (a_L) dispersivity of the porous/fractured medium (m). ALPHAL is different from the colloid longitudinal dispersivity, which will be read in the data block TRACR
ALPHAT	The solute transverse (a_T) dispersivity of the porous/fractured medium (m). ALPHAT is different from the colloid transverse dispersivity, which will be read in the data block TRACR
TRANCO	The dimensionless transfer coefficient K_t between the mobile and the immobile water phases.
PHIF	The bulk fracture porosity of a fracture, defined as the ratio of the fracture pore volume to the sum of the fracture and matrix pore volumes. This parameter is needed in dual permeability simulations of fractured rocks, and is needed to accurately compute diffusive and dispersive fluxes.

Card ROCKS.1.1 is necessary in EOS9nT. Even if NAD = 0 in ROCKS.1, the code resets it internally to 1, and attempts to read the data values. For NAD $\geq$ 1, there is no change. If the fields for ALPHAL and ALPHAT are left blank, zero values are assigned.

The user is cautioned that the tortuosity TORT in card ROCKS.1.1 (i.e., the τ parameter) is important in the simulation of tracer transport, and that representative values should be used especially under diffusion-dominated regimes. Leaving the TORT field blank sets TORT = 0.0, and eliminates molecular diffusion in the simulation. The tortuosity of the surface diffusion paths τ_s is computed internally as $\tau_s = \tau$.

5.1.3. Domain REFCO

EOS9nT allows providing reference conditions through the use of a ficticious domain (rock) named REFCO. If a REFCO domain is present in rocks, then:

(a) If DROK $\neq$ 0.0, the reference gas pressure P_g = DROK.

(b) If POR $\neq$ 0.0, the reference temperature T = POR.

(c) If PER(1) $\neq$ 0.0, the reference water density ρ = PER(1).

(d) If PER(2) $\neq$ 0.0, the reference water viscosity μ = PER(2).

(e) If PER(3) $\neq$ 0.0, the reference water compressibility b_w = PER(3).

(f) If CWET $\neq$ 0.0, the reference elevation for gravity-capillary equilibrium z = CWET. When CWET $\geq 10^5$ in domain REFCO, then gravity equilibration is performed using the watertable elevation read as part of the ELEME data block (a thorough discussion is presented in Section 5.3.1).

(g) If SPHT $\neq$ 0.0, it specifies an optional index number of irreducible water saturation; this will cause water saturation to be specified at the irreducible level for strong capillary pressures.

If no REFCO domain is present, then the default initial conditions are: $P_g = 1.0103 \times 10^5$ Pa and $T = 15°$C.

5.1.4. Domain SEED

When a domain SEED is present, modifiers (multipliers) will be applied to the permeabilities k, and *Leverett* [1941] scaling will be applied to the capillary pressures P_c. Denoting the permeability modifier with k_m, the modified permeability k^* becomes

$$k^* = k_m\, k \ , \tag{65}$$

and the scaled capillary pressure P_c^* is given by

$$P_c^* = \frac{P_c}{\sqrt{k_m}} \tag{66}$$

The following options are available:

(a) When DROK=POR=0.0 in domain SEED, the parameters PMX read as part of the ELEME data block will be used as modifiers. However, when a file RANDOM is present, 10,000 PMX data will be read from it, overwriting the ELEM data.

(b) When DROK≠0, random numbers will be generated internally with DROK as seed. A linear permeability modification will be made.

(c) When DROK=0 and POR≠0, random numbers will be generated internally with POR as seed. A logarithmic permeability modification will be made.

In domain SEED, PER(1) is an optional scale factor. Random numbers will be generated in the interval (0, PER(1)). If w is a random number ($0 \leq w \leq 1$), the permeability modifiers k_m are:

(a) k_m = PMX, when PMX are externally supplied

(b) k_m = PER(1) *w, when DROK≠0 (linear scaling)

(c) k_m = exp(-PER(1) *w), when DROK=0.0 and POR≠0 (logarithmic scaling)

PER(2) is an optional shift: for PER(2)≠0, the permeability modifiers used are $k_m = k_m$ - PER(2).

5.2. Data Block PARAM

5.2.1. Card PARAM.1

In EOS9nT, the computational parameters read in PARAM.1 are:

```
NOITE,KDATA,MCYC,MSEC,MCYPR,(MOP(I),I=1,24),
                DIFF0,TEXP,BE,ITRACR
```

and the format is

```
FORMAT(2I2,3I4,24I1,3E10.4,I2)
```

All the parameters in PARAM.1 are as defined in [*Pruess*, 1987]. The new parameter ITRACR= n, i.e., the number of tracers under consideration. If ITRACR(≠0) differs from NTRACR in the data block TRACR in Section 5.4, a warning of the discrepancy is printed and the simulation is aborted.

The parameters MOP(23) and MOP(24) are important in EOS9nT because their use can significantly reduce execution times.

5.2.1.1. The MOP(23) parameter. If MOP(23)=9 and the file UNVEC exists, then EOS9nT does not compute the unit vectors normal to the gridblock interfaces, but instead reads this information, as well as information on the indices of the neigbors to each element involved in the connections.

If the UNVEC file does not exist or MOP(23)≠9, EOS9nT creates the UNVEC file. Because the parameters in UNVEC are not easy to determine, this file must always be created by an EOS9nT run. Note that the existence of the UNVEC file can drastically reduce execution times. In our experience from 3-D simulations involving grids of 100,000 gridblocks, this option can reduce execution times by about 65%. If the same grid is used for more than one simulations, the user is strongly urged to use this option.

It is important, however, to ensure that MOP(23)≠9 and/or no UNVEC file be present when the first simulation is attempted. Failure to do so can lead to serious problems if the domain geometry implicit in UNVEC is in conflict with the one in the input file.

5.2.1.2. The MOP(24) parameter. If MOP(24)=9 and the file VELOC exists, then EOS9nT does not solve the fow equations, but instead reads from VELOC the water flux, pore velocity, Darcy velocity, interface area, and upstream weighting factor at each connection.

As in the case of MOP(23), if the VELOC file does not exist or MOP(23)≠9, EOS9nT creates the VELOC file. The user is sytrongly advised against attempting to develop this file, which should always be created by an EOS9nT run. In conjunction with an UNVEC file, the presence of VELOC reduces execution times. If the same steady-state flow field is used for more than one simulations, the user is strongly urged to use this option.

It is important, however, to ensure that MOP(24)≠9 and/or no VELOC file be present when (a) the first simulation is attempted and/or (b) the flow field is not time-invariant.

Failure to do so can lead to serious problems if the domain geometry and/or the flow field in VELOC is in conflict with the ones in the input file.

5.2.2. Card PARAM.4

This card holds the primary variable DEP(1) which is used as default initial conditions for all elements not specified in the data block INCON if the option START is selected.

In EOS9nT, the card PARAM.4 may hold one of the following:

(a) The water pressure P: DEP(1) $\geq$ 1.

(b) The water saturation: 0 $\leq$ DEP(1) $<$ 1.

(c) The capillary pressure: DEP(1) $<$ 0.

Initialization of EOS9nT is possible using any of these three option. Additionally, initialization is possible from gravity-capillary pressure equilibrium based on elevation from the watertable (an input). This last option is discussed in Sections 5.1.3 and 5.3.1.

5.2.3. Cards PARAM.4.1, PARAM.4.2, PARAM.4

These cards are mandatory if ITRACR$\neq$0, in which case they holds (a) the default initial mass fractions X_i of the ITRACR tracers in the water, (b) the initial primary component of the sorbed or filtered mass, and (c) the initial secondary component of the sorbed or filtered mass (for combined sorption), respectively, i.e.,

```
TMASSF(I), I=1,...,ITRACR
XSOFIL(I), I=1,...,ITRACR
XSOFI2(I), I=1,...,ITRACR
```

according to the format

```
FORMAT(4E20.13)
```

Note that the Card(s) PARAM.4 are mandatory, regardless of whether secondary sorption is considered in the simulation.

5.3. Data Block ELEME

5.3.1. Card ELEME.1

In EOS9nT, the element information in `ELEME.1` can use the output of the MESHMAKER facility (module MESHM), but includes some additional information. More specifically, the following information is provided in `ELEME.1`:

```
ELEM,MA1,MA2,VOLX,PMX,ZREF,XX,YY,ZZ
```

and the format is

```
FORMAT(A5,10X,A3,A2,6(E10.4))
```

These parameters are defined as follows:

`ELEM`	The element name.
`MA1,MA2`	A five character material identifier corresponding to one of the domains (rocks) in data block ROCKS. If the first 3 characters are blank, the last two characters must be numbers, in which case they indicate the sequence number of the domain as entered in ROCKS.
`VOLX`	Element volume (m^3).
`PMX`	Permeability modifier (see Section 5.1.4) for statistical heterogeneity applications.
`ZREF`	Reference watertable elevation for gravity-capillarity equilibration (m). It is invoked when the ZREF parameter in the REFCO domain (data block ROCKS) is $\geq 10^5$. Areally-variable watertable elevations can thus be entered.
`XX`	x-coordinate of the gridblock center, with respect to a global coordinate system (m).
`YY`	y-coordinate of the gridblock center, with respect to a global coordinate system (m).
`ZZ`	z-coordinate of the gridblock center, with respect to a global coordinate system (m).

The PMX and ZREF fields may be blank. However, care must be taken to provide accurate information in the XX, YY and ZZ fields. This information is needed to determine

the unit vectors at the centers of the two elements across each connection, which are used to determine the dispersion tensor. Inaccurate coordinate information will lead to erroneous results.

5.4. Data Block TRACR

This is a new data block required by EOS9nT. It provides all the necessary information on the tracers and their treatment. It includes the following cards:

5.4.1. Card TRACR.1

The following information is provided in `TRACR.1`:

```
NTRACR,MXTRDT,NOITTR,FLOWFI,LPLACE,
LPTYPE,NITR,CRLAPL,NOPRNT
```

according to the format

```
FORMAT(3(I5),4X,A6,I1,A4,I2,3X,E10.4,I2)
```

These parameters are defined as follows:

`NTRACR`	The number of tracers. If `ITRACR`$\neq$0 in `PARAM.1` and `ITRACR` $\neq$`NTRACR`, then a warning message will be printed and the simulation will be aborted.
`MXTRDT`	The maximum allowable number of timesteps in the solute transport simulation. It refers to the highest number from among all the tracers. If `MXTRDT` is left blank, it is reset to 99999. If `MXTRDT`$\neq$ 0 but `MXTRDT` < `MCYC`, then `MXTRDT` is reset to `MXTRDT` = `MXTRDT+MCYC`.
`NOITTR`	The maximum allowable number of Newtonian iterations for the solution of the transport equation (applies for conventional timestepping only). If `NOITTR` is left blank, it is reset to 5.

FLOWFI — The status of the flowfield. If FLOWFI='steady', then the flow equation is solved only once to obtain the required velocities and mass fluxes across the element connections. Only the solute equations are then solved. If FLOWFI≠'steady', FLOWFI is reset internally to 'transi', and both the flow and transport equations are solved.

LPLACE — If LPLACE=1, then, after the flow field becomes time-invariant, the transport equations are solved using a Laplace transform formulation. For LPLACE≠1, conventional timestepping is employed in the solution of the tracer equations.

LPTYPE — The algorithm for the numerical inversion of the Laplace space solutions. There are two option:

LPTYPE ='stfs' : The Stehfest algorithm is used

LPTYPE ='hoog' : The Hoog algorithm is used

If LPTYPE≠'stfs' and LPTYPE≠'hoog', a warning is printed and the simulation is aborted

NITR — The number of summation terms in the algorithms for the numerical inversion of the Laplace space solutions.

For LPTYPE='stfs', NITR is the N_s term in equation (31). It must be an even integer, and 10≤NITR ≤ 18. If NITR < 10 or NITR > 18, or is left blank, it is reset internally to the default value of 18. If an odd number between 10 and 18 is entered, NITR is reset internally to the next larger integer value.

For LPTYPE='hoog', NITR is the M_H term in Section 3.2.3. It is an integer, and 5≤NITR ≤ 10. If NITR < 5, NITR > 10, or is left blank, it is reset internally to the default value of 6.

CRLAPL — The convergence criterion for the conjugate gradient solution in the Laplace space. Because a very accurate solution must be obtained in the Laplace space to ensure accurate solutions in time, the convergence criterion must be much tighter than for the flow equation. If CRLAPL > 10^{-9}, CRLAPL < 10^{-14}, or is left blank, it is reset internally to the default value of 10^{-10}.

NOPRNT — If NOPRNT≠0, only the mass and volume balances of phases and tracers are printed. Otherwise, the distributions in the domain are also printed (default NOPRNT = 0). This is a useful feature for breakthrough studies in very large grids.

If NTRACR=0, no additional cards are read in the TRACR data block, and the simulation is conducted without considering any tracers, i.e., only the flow equation is solved.

5.4.2. Card TRACR.2

The following variables are read in TRACR.2:

IFFACT, ISFACT, IDFACT, ICOVRD, ITOVRD, COURAN, HLFRAC

according to the format

FORMAT(5(I1,1X),2(E10.4))

These parameters are defined as follows:

IFFACT — Indicator for flow velocity averaging (default IFFACT=0). It is not applicable when the Laplace transform formulation is invoked.

- IFFACT=0 : The flow velocity is interpolated at the midpoint of the transport $\Delta t_{t,i}$.
- IFFACT=1 : The flow velocity is interpolated at the end of the transport $\Delta t_{t,i}$.
- IFFACT=2 : The flow velocity is interpolated at the midpoint of the flow Δt_f.
- IFFACT=3 : The flow velocity is interpolated at the end of the flow Δt_f.

ISFACT — Indicator for water saturation averaging (default ISFACT=0). It is not applicable when the Laplace transform formulation is invoked.

- ISFACT=0 : The water saturation is interpolated at the midpoint of the transport $\Delta t_{t,i}$.
- ISFACT=1 : The water saturation is interpolated at the end of the transport $\Delta t_{t,i}$.
- ISFACT=2 : The water saturation is interpolated at the midpoint of the flow Δt_f.
- ISFACT=3 : The water saturation is interpolated at the end of the flow Δt_f.

IDFACT — Indicator for radiactive decay averaging (default IDFACT=0). It is not applicable when the Laplace transform formulation is invoked.

- IDFACT=0 : The decay is applied to the tracer concentration at the end of the transport $\Delta t_{t,i}$ (default).
- IDFACT=1 : The decay is applied to the tracer concentration at the midpoint of the transport $\Delta t_{t,i}$.

ICOVRD — Indicator for overriding the default Courant number (the default value of ICOVRD=0). It is not applicable when the Laplace transform formulation is invoked.

- ICOVRD$\neq$9 : The Courant number is reset to the default (=1) if it exceeds 1.
- ICOVRD=9 : The Courant number is not reset to the default (=1) if it exceeds 1, but the value in COURAN is used.

ITOVRD — Indicator for overriding the default half-life fraction for $\Delta t_{t,i}$ limitation (default ITOVRD =0). It is not applicable when the Laplace transform formulation is invoked.

- ITOVRD$\neq$9 : The half-life fraction is reset to the default (=0.1) if it exceeds 0.1.
- ITOVRD=9 : The half-life fraction is reset to the default (=0.1) if it exceeds 0.1, but the value in HLFRAC is used.

COURAN — The maximum allowable Courant number (default COURAN = 1.0). It is not applicable when the Laplace transform formulation is invoked. If COURAN $\leq$ 0 or COURAN > 1, COURAN is reset to COURAN =1.0. If COURAN > 1 and ICOVRD = 9, COURAN is not reset but remains as specified.

HLFRAC — The maximum allowable fraction of the tracer half-life (if radioactive) for limiting $\Delta t_{t,i}$ (default HLFRAC = 0.1). It is not applicable when the Laplace transform formulation is invoked. If HLFRAC $\leq$ 0 or HLFRAC > 0.1, HLFRAC is reset to HLFRAC = 0.1. If HLFRAC >0.1 and ITOVRD=9, HLFRAC is not reset but remains as specified.

5.4.4. Cards TRACR.3.1, TRACR.3.2, TRACR.3.2.1 and TRACR.3.3

These are read according to the following format:

```
do n=1,NTRACR
    read TRACR.3.1
    do i=1,NMROCK (on Card TRACR.3.1 - defined below)
        read TRACR.3.2
            If TRTYPE='C',read TRACR.3.2.1
        read TRACR.3.3
    end do
end do
```

The parameters on card TRACR.3.1 are:

TRACER,TRTYPE,PCTYPE,NMROCK,IDROCK,NDAUTR,NADDID,

IDPARE,IDSEQ,MATCOL,DD00,HAFLIF,WTMOL,ZETA,RHOCOL

and the corresponding format is

```
FORMAT(A5,A2,A1,7(i3),1x,5(e10.4))
```

5.4.4.1. The parameters in Card TRACR.3.1. These are defined as follows:

TRACER	The tracer name.	
TRTYPE	The type of tracer. For pseudocolloids, TRTYPE='PC'; for true colloids, TRTYPE='TC'; for solutes, TRTYPE='SO' (default).	
PCTYPE	PCTYPE = 'P':	Designates a decaying radioactive parent
	PCTYPE = 'D':	Designates a daughter product of radioactive decay
	PCTYPE = 'S':	Designates colloid-assisted transport
	PCTYPE = 'N':	Non-radioactive substance, or no colloid-assisted transport

NMROCK — The number of domains for which sorption coefficients are provided.

IDROCK — If NMROCK is less than the total number of domains in the data block ROCKS, then the properties of the remaining domains will be set equal to those of the domain with the IDROCK sequence number (i.e., the order in which the rock type is read in the data block ROCKS). If IDROCK$\leq$0 or IDROCK > number of rock domains, the domains about which no sorption data are provided are assumed to be non-sorbing.

NDAUTR — Number of daughter products. It is necessary if PCTYPE='P'.

NADDID — The additive group index of daughter products of radioactive decay. This feature allows accounting for the cumulative effects of daughter products produced from different radioactive decay chains. In EOS9nT each daughter product of radioactive decay is treated individually, although the same radionuclide may be produced from two different parents. For example, if tracers 3 and 6 are the same daughter produced from the decay of two different parents, their group number is NADDID=1 for both. Similarly, if tracers 4, 9 and 11 are the same daughter from different parents, their group number is NADDID=2. When NADDID$\neq$0, upon printout the concentrations in the liquid and in the solid of the last member of the group (i.e., of tracer 11 for NADDID=2) are the cumulative concentrations of the daughter.

IDPARE — Parent identifier. It is necessary if PCTYPE='D'.

IDSEQ — The decay sequence number of the daughter in the radioactive decay chain. It is necessary if PCTYPE='D'.

MATCOL — The rock number corresponding to the colloid (requires entering the colloid as a material in ROCKS). This is needed for colloid-assisted transport, i.e., when TRTYPE='PC'.

DD00 — The tracer molecular diffusion coefficient (m^2/s).

HAFLIF — The tracer half life (s). If the field is left blank, HAFLIF is reset internally to the default (= 10^{50} s). If HAFLIF<0 and PCTYPE='P' or PCTYPE='D', ABS(HAFLIF) is the $\mathcal{K}$ of the reaction in equation (17).

WTMOL — The molecular weight of the tracer. It is necessary if the daughter of the tracer is tracked.

ZETA	The fraction of the mass of the decayed sorbed parent that remains sorbed as a daughter ($0 \leq \zeta_\nu \leq 1$). The term ζ_ν is introduced to account for the different sorption behavior of parents and daughters, and the fact that daughters can be ejected from grain surfaces due to recoil, e.g., the ejection of ^{234}Th from grain surfaces during the alpha decay of ^{238}U [*Faure*, 1977]. ζ is only important when sorption does not follow an equilibrium isotherm. The default $\zeta = 1$.
RHOCOL	The colloid density (kg/m^3). This is needed when TRTYPE$\neq$'SO'

5.4.4.2. The parameters in Card TRACR.3.2. A total of NMROCK cards TRACR.3.2 are read. The parameters on the cards are:

```
NNROCK,NSORTP(NNROCK,n,1),NSORTP(NNROCK,n,2),
    NSORTP(NNROCK,n,2),NOSAME(NNROCK)
(SKD(NNROCK,1,n,j), j=1,...,6),DDSS(NNROCK,n)
```

and the corresponding format is

```
FORMAT(I3,1X,I1,I1,1X,I3,7(e10.4))
```

where n is the tracer number for which sorption and filtration parameters are read. These parameters are defined as follows:

NNROCK	The sequence number of the rock domain, of which the sorption properties will be read immediately after.
NSORTP(NNROCK,1):	A flag indicating the type of sorption of tracer n on the rock/soil i. = 1: Linear equilibrium sorption (physical) = 2: Langmuir equilibrium sorption (physical) = 3: Freundlich equilibrium sorption (physical) = 4: Linear kinetic sorption (physical) = 5: Langmuir kinetic sorption (physical) = 6: Freundlich kinetic sorption (physical) = 7: Linear kinetic chemical sorption = 8: Colloid equilibrium filtration = 9: Colloid kinetic filtration and declogging

NSORTP(NNROCK,2): A flag indicating the presence of combined sorption of solute n on the rock/soil i. NSORTP(NNROCK,2)=0 indicates no combined sorption or filtration. Otherwise, it denotes the second type of the combined sorption or filtration.

= 1: Linear equilibrium sorption (physical)
= 2: Langmuir equilibrium sorption (physical)
= 3: Freundlich equilibrium sorption (physical)
= 4: Linear kinetic sorption (physical)
= 5: Langmuir kinetic sorption (physical)
= 6: Freundlich kinetic sorption (physical)
= 7: Linear kinetic chemical sorption
= 8: Colloid equilibrium filtration
= 9: Colloid kinetic filtration and declogging

NOSAME(NNROCK) The number of additional rock/soil domains that have the same properties with domain NNROCK.
If NOSAME(NNROCK) $\neq$0, then the domain numbers of NOSAME(NNROCK) additional rocks/soils will be read in card(s) TRACR.3.3 immediately after the card TRACR.3.2.

DDSS The tracer surface diffusion coefficient (m^2/s). DDSS is reset internally to DDSS=0 when TRTYPE='S'.

Defining N_1 = NSORTP((NNROCK,1)) and N_2 = NSORTP((NNROCK,2)),

SKD(NNROCK,1)
For N_1 = 1 or 4: K_d (in m^3/kg): distribution coefficient of the linear equilibrium sorption of tracer i onto domain number NNROCK – see equations (12) and (13).

For N_1 = 2 or 5: K_1 (in m^3/kg): coefficient of the Langmuir equilibrium sorption of tracer i onto domain number NNROCK – see equations (12) and (13).

	For $N_1 = 3$ or 6	K_F (in m^{-b}/kg^{3b}): coefficient of the Freundlich equilibrium sorption of tracer `i` onto domain number NNROCK – see equations (12) and (13).
	For $N_1 = 7$	k_c^+ (in 1/s): the forward kinetic coefficient of the chemical sorption of solute `i` onto domain number NNROCK – see equation (15).
	For $N_1 = 8$ or 9	K_σ (in m^3/kg): distribution coefficient of the linear equilibrium deposition of colloid `i` onto domain number NNROCK – equations (19) and (20).
SKD(NNROCK,2)	For $N_1 = 1, 4, 8$	Set to zero internally (not used).
	For $N_1 = 2$ or 5	K_2 (in m^3/kg): coefficient of the Langmuir equilibrium sorption of tracer `i` onto domain number NNROCK – see equations (12) and (13).
	For $N_1 = 3$ or 6	b (dimensionless): exponent of the Freundlich equilibrium sorption of tracer `i` onto domain number NNROCK – see equations (12) and (13).
	For $N_1 = 7$	k_c^- (in 1/s): the backward kinetic coefficient of the chemical sorption of solute `i` onto domain number NNROCK – see equation (15).
	For $N_1 = 9$	κ^+ (in 1/s): kinetic clogging coefficient of filtration of colloidal tracer `i` through domain number NNROCK – see equation (13).

SKD(NNROCK,3)	For N_1 = 1,2,3,7,8	Set to zero internally (not used).
	For N_1 = 4	k_ℓ (in 1/s): the kinetic constant of the linear kinetic sorption of tracer i onto domain NNROCK – see equation (13).
	For N_1 = 5	k_L (in 1/s): kinetic constant of the Langmuir kinetic sorption of tracer i onto domain NNROCK – see equation (13).
	For N_1 = 6	k_F (in 1/s): kinetic constant of the Freundlich kinetic sorption of tracer i onto domain number NNROCK – see equation (13).
	For N_1 = 9	κ^- (in 1/s): kinetic declogging coefficient of filtration of colloidal tracer i through domain number NNROCK – see equation (20).

For solute transport, SKD(NNROCK,4),SKD(NNROCK,5) and SKD(NNROCK,6) describe the same parameters as SKD(NNROCK,1), SKD(NNROCK,2) and SKD(NNROCK,3), respectively, and pertain to the second type of sorption in combined sorption.

5.4.4.3. The parameters in Card TRACR.3.2.1. For colloid filtration (TRTYPE='TC' or 'PC'), the card TRACR.3.2 is followed by card TRACR.3.2.1, which includes the parameters

ALPHCL,ALPHCT,COVLFA,COLEFF,ENTRFR,COLDIA,PORDIA,PERKM

These are read according to the format

FORMAT(8(E10.4))

and are defined as follows:

ALPHCL	The colloid longitudinal dispersivity α_L (in m).
ALPHCT	The colloid transverse dispersivity α_T (in m). ALPHCL and ALPHCT are different from that for the solutes (read in the data block ROCKS, and their magnitude may depend on the colloidal particle size.
COVLFA	The colloid velocity adjustment factor s in equation (21). If COVLFA >1.5 or COVLFA<1, it is reset internally to 1 (default).
COLEFF	The single collector efficiency α_c of equation (22).
ENTRFR	The colloid accessibility factor f_c (see Section 2.3.7.3).
COLDIA	The colloid diameter d_c (in m) in equation (23).
PORDIA	The particle grain diameter or the fracture aperture d_m (in m) in equation (23).
PERKM	A parameter describing the kinetic reverse (declogging) filtration coefficient κ^- (in 1/s) in equation (20). If PERKM$\geq$ 0, κ^- = PERKM; if PERKM$<$ 0, then it represents the ratio κ^-/κ^+, from which κ^- = $\kappa^- \times$ ABS (PERKM). This approach maintains a dependence of κ^- on the flow velocity akin to that of κ^+ and is conceptually sounder than the constant value approach.

5.4.4.4. Options for describing filtration in EOS9nT. Equilibrium fitration in EOS9nT is handled by setting N_1 (and N_2, if secondary filtration is considered) to 8 (see Section 5.4.4.2). There are two ways to handle kinetic filtration, depending on the expression used to describe κ^+ in equation (21).

If the first expression in equation (21) is used, then the kinetic filtration parameters are obtained by setting N_1 (and N_2, if needed) to 9, and providing the appropriate SKD values (see Section 5.4.4.2). If the second exression in (21) is used, then the necessary parameters are provided by the data in Card 3.2.1 (Section 5.4.4.3).

It is important to describe how the filtration coefficient are used, as the simulation of colloids requires both Card 3.2 and Card 3.2.1. These two cards provide the information needed for both expressions in equations (21).

The key to the selection of the appropriate κ^+ model is the value of COLEFF. Setting COLEFF=0.0 ensures that κ^+ is obtained from the first model in (21). For COLEFF$\neq$0.0, the velocity-dependent κ^+ model is applied. Note that a nonzero value of COLEFF resets N_1 internally to 9 regardless of its initial input value.

5.4.4.5. The parameters in Card TRACR.3.3. The parameters on card TRACR.3.3 are:

(NOROCK(NNROCK,j), j=1,...,NOSAME(NNROCK))

and the corresponding format is

FORMAT(16(I5))

NOROCK is the domain number of rocks/domains that have the same properties with domain NNROCK.

5.4.4.6. Important issues. As it has already been discussed, the Laplace transform formulation can only be applied when sorption is described by a linear equilibrium or kinetic process. Therefore, if NSORTP $\neq$, NSORTP $\neq$ 4, ETA1 $\neq$ 0 or ETA2 $\neq$ 0, the parameter LPLACE in Card TRACR.3.2 is reset internally to zero, and conventional timestepping is employed.

In preparing the data set TRACR, the user must keep in mind that the order of listing of the tracers is important because it defines the computation order of the solutions for each of the tracers. The data cards of the members of a radioactive decay or reaction chain must be listed consecutively. This is because EOS9nT stores the solutions of the parents for the computation of the solutions of the daughters. Because of the sequential nature of the tracer solutions in EOS9nT, the stored solution from the previous species will not correspond to the correct daughter if parents and daughters are not in order.

If the study includes solutes and colloid-assisted transport on more than one pseudo-colloids, it is important to first list the cards with the parameters of all the colloids, and

follow them with the cards with the solute properties. This allows accurate computation of the sorbed mass onto the colloids in the summation of equation (24).

5.5. Data Block INCON

5.5.1. Card INCON.1

The computational parameters read in INCON.1 are:

```
EL,NE,NSEQ,NADD,PORX,KTRACR
```

and the format is

```
FORMAT(A3,I2,2I5,E15.8,I2)
```

All the parameters in INCON.1 are as defined in [*Pruess*, 1987; 1991]. The new parameter KTRACR= n, i.e., the number of tracers under consideration. If KTRACR($\neq 0$) differs from NTRACR in the data block TRACR in Section 5.4, a warning of the discrepancy is printed and the simulation is aborted.

5.5.2. Cards INCON.3, INCON.4 and INCON.5

These new cards (or sets of cards, if the number of tracers ≥ 4) INCON.3 and INCON.4 read the (a) initial mass fractions of the tracers, (b) the initial primary sorbed or filtered (for colloids) concentrations, and (c) the initial secondary sorbed or filtered (for colloids) concentrations (for combined sorption), respectively , i.e.,

```
TMASSF(I),  I=1,...,max{NTRACR,ITRACR}
XSOFIL(I),  I=1,...,max{NTRACR,ITRACR}
XSOFI2(I),  I=1,...,max{NTRACR,ITRACR}
```

according to the format

```
FORMAT(4E20.13)
```

The use of max{NTRACR, ITRACR} is necessitated by the ability of TOUGH2 to

read the input data blocks in an arbitrary order. Thus, there is no guarantee that the number of tracers will have been read in PARAM (ITRACR) or TRACR (NTRACR) when the INCON data are read. Although this approach provides an extra level of redundancy, there is still a possibility of a problem if INCON is read before the PARAM and TRACR data blocks. Thus, it is important to ensure that these data blocks are read before INCON.

Note that in EOS9nT all the equations are linear with respect to concentration. Thus, any value can be used as the initial TMASSF, to be changed later by multiplying by an appropriate factor. It is convenient to use TMASSF=1.

5.6. Data Block INDOM

5.6.1. Card INDOM.1

The computational parameters read in INDOM.1 are:

```
NAM, KTRACR
```

and the format is

```
FORMAT(A5, I2)
```

The parameter NAM in INDOM.1 is as defined in [*Pruess*, 1987; 1991]. The parameter KTRACR= n, i.e., the number of tracers under consideration. If KTRACR($\neq 0$) differs from NTRACR in the data block TRACR in Section 5.4, a warning of the discrepancy is printed and the simulation is aborted.

5.6.1. Cards INDOM.3, INDOM.4 and INDOM.5

These new cards (or sets of cards, if the number of tracers ≥ 4) INDOM.3 read (a) initial mass fractions of the tracers, (b) the initial primary sorbed or filtered (for colloids) concentrations, and (c) the initial secondary sorbed or filtered (for colloids) concentrations (for combined sorption), respectively , i.e.,

TMASIN(I), I=1,...,max{NTRACR,ITRACR}

XSOFIN(I), I=1,...,max{NTRACR,ITRACR}

XSOF2N(I), I=1,...,max{NTRACR,ITRACR}

according to the format

FORMAT(4E20.13)

Because of the reasons discussed in the previous section (4.5), it is important to ensure that the PARAM and TRACR data blocks are read before INDOM.

5.7. Data Block GENER

5.7.1. Card GENER.1

This card is modified to read the following parameters:

EL,NE,SL,NS,NSEQ,NADD,NADS,LTAB,TYPE,ITAB,GX,EX,HX,NTRQ

according to the format

FORMAT(A3,I2,A3,I2,4I5,5X,A4,A1,3E10.4,I2)

NTRQ is the only addition, and all the other parameters remain as defined in *Pruess* [1987]. NTRQ is the number of tracers, and is only important if GX $\geq$ 0.0, i.e., only for injection. NTRQ is internally checked against NTRACR and ITRACR, and the simulation is aborted (after printing a warning message) if a discrepancy is detected..

5.7.2. Card GENER.1.0.1

This new card (or cards, if NTRQ $\geq$ 4) is (are) read immediately after GENER.1 only when GX $\geq$ 0.0, and includes the parameters.

TMFQ(I), I=1,...,NTRQ

These are read according to

FORMAT(4E20.13)

The parameter TMFQ(I) is the mass fraction of tracer I in the injection stream when TMFQ(I)>0. When it has a negative value, ABS(TMFQ(I)) represents the actual mass injection rate of tracer I in kg/s.

5.7.3. Card GENER.1.3

The heat equation is not solved in EOS9nT. The GENER.1.3 card (or cards) is (are) thus used to read the mass fractions of the tracers in the injection streams in a tabular form, i.e.,

```
F3(L), L=1,...,NTRACR*LTAB
```

according to

```
FORMAT(4E20.13)
```

If the declared size of F3 is insufficient, then a warning message is printed and the simulation is aborted. An important point is that to implement the Laplace transform formulation, the injection mass rate GX must be constant over time. If GX is time-variant, the Laplace transform formulation can still be employed if its time dependence can be described by a time function with a known Laplace transform. In this case, however, the user will have to modify subroutine LQTRCR (for the Stehfest alhorithm) and/or HQTRCR (for the De Hoog algorithm) by adding the code for the Laplace transform of the injection rate.

5.8. Options for Very Large Grids

When the grid exceeds 100,000 elements, problems arise if the conventional TOUGH2 options [*Pruess*, 1991] are employed. These problems surface when TOUGH2 creates the external MESH and GENER files for subsequent transport simulations involving the same domain and source/sink set.

5.8.1. Problems in the MESH File

After reading the element and connection data, TOUGH2 creates the MESH file, at the end of which it attaches the indices of the elements in all the grid connections. These indices allow computational economy in subsequent runs because TOUGH2 does not spend the time needed for their determination (a considerable task in large grids). The conventional TOUGH2 writes these indices according to a `16(I5)` format. For grids $\geq$100,000 elements, this format is inadequate because larger fields are required. Thus, the created MESH file is erroneous and cannot be further used.

5.8.2. Problems in the GENER File

A similar problem arises in the creation of GENER. After reading the element names at which sinks and sources are located, conventional TOUGH2 determines the corresponding element numbers and attaches them at the end of the GENER file using the same `16(I5)` format. In large grids involving a large number of sources, the associated computational effort is significant. The corresponding time savings by reading (rather than determining) the source/sink element numbers from the GENER file cannot be realized when the grid $\geq$100,000 elements because their numbers are incorrectly stored.

5.8.3. Addressing the Problems

The problem is eliminated by attaching the `ext1` keyword at the end of the ELEME and GENER keywords. Thus, the new keywords at the top of the ELEME and GENER data blocks become `ELEMEext1` and `GENERext1`, respectively. When EOS9nT reads the `ext1` keyword, the element indices at the end of the MESH and GENER files are stored using a `10(I8)` format.

The same keywords cause the parameters

```
EL,NE,NSEQ,NADD,MA1,MA2,VOLX,AHTX,ZREF,X,Y,Z
```

in the Card ELEME.1 of the ELEME data block (see Section 5.3.1) to be read according to the format

```
A3,I2,2I5,A3,A2,3E10.4,2F10.3,F10.4
```

This format is useful for simulations involving large distances in the simulation domains. For example, studies of radionuclide transport at the site of the proposed high-level radioactive waste repository in Yucca Mountain, Nevada, involve state coordinates that are accommodated using this format.

6. Outputs

6.1. Output Description and Output Control

EOS9nT can provide the following output:

1. The standard general information outputs of the TOUGH2 family of codes [*Pruess*, 1991].
2. The options and general tracer transport information discussed in Sections 5.1, 5.2, and 5.4.
3. The pressure (in Pa), saturation, capillary pressure (in Pa), the relative permeability and diffusivity of the liquid phase in the gridblocks of the domain.
4. The flux (in kg/s) and velocity (in m/s) of the liquid phase across the gridblock interfaces (connections) of the domain.
5. The primary variable (pressure or saturation) and its changes in the gridblocks of the domain.
6. The mass fractions of the n tracers in the water phase (in kg/kg), and the corresponding physically and chemically sorbed (for solutes) or filtered (for colloids) concentrations

(in kg/m^{-3} of medium), as well as (c) the reacted mass fractions in the water phase (in kg/kg) in the gridblocks of the domain.

7. The diffusive, advective and total fluxes of the n tracers (in kg/s) across the gridblock interfaces of the domain.
8. Volume and mass balances of the liquid and gas phases in the domain (in m^3 and kg, respectively), and mass balances of the n tracers (in kg).
9. The standard output files printed by TOUGH2 [*Pruess*, 1987;1991].

Of those possible outputs, (1), (2), (8) and (9) are always printed. To obtain output of volume and mass balance data only, the parameter NOPRNT in card 4.1 (see Section 5.4.1) is set to a non-zero integer. For (3) and (6) to be printed, the parameter KDATA in the data block PARAM must be ≥ 1 (default $= 1$). For (4) and (7) to be printed, KDATA must be ≥ 2. For (5) to be printed, KDATA must be 3. In keeping with the TOUGH2 convention [*Pruess*, 1987], if the KDATA values are increased by 10, printouts will occur after each iteration (not just after convergence).

Note that when the flowfield is or becomes time-invariant (i.e., when the parameter `FLOWFI='steady'` in card 4.1, see Section 5.4.1), (3), (4) and (5) are printed only once. After this point, only the transport equations are solved, and thus only the transport outputs (6), (7) and (8) are printed.

6.2. Warning Messages

If inputs indicate conflicting conditions and/or parameter values are outside realistic ranges, EOS9nT is designed to respond according to the severity of the violation. Non-critical conflicts result in a warning or clarifying message, internal adjustment of the corresponding conditions and/or parameters, and continuation of the simulation. Serious

violations result in an error message identifying the problem, and the simulation is aborted.

Warnings are printed, and the corresponding internal adjustments are made, in the following cases:

1. The number of rocks/soils for which sorption parameters are provided is larger than the number NM in data block ROCKS. Then only the sorption of the first NM rocks are used, and the rest are ignored.
2. If a rock/soil porosity PHI>2 in ROCKS, it represents an 'atmospheric' domain, and its tortuosities and dispersivities are reset to 0.
3. A gridblock has no domain assignment. Then the properties of domain 1 are assigned to the gridblock.
4. The number of significant digits is between 9 and 12. The message warns the user to expect deteriorating convergence behavior.
5. The number of significant digits in double precision arithmetic is equal or less than 8. The message warns the user of insufficient significant digits, potential convergence failure, and the need to employ double precision arithmetic.
6. There are no tracers in the system (cc NTRACR=0). Then only the flow equation will be solved.
7. If ITRACR≠0 in PARAM and the data block TRACR is missing, ITRACR is reset to 0, and only the flow equation is solved.
8. If MXTRDT≤0 (see data block TRACR), it is reset to 99999 (default).
9. If FLOWFI≠'TRANSI' and FLOWFI≠'STEADY' (see data block TRACR), FLOWFI is reset to 'STEADY' (default).
10. If the flag for the Laplace transform formulation LPLACE<0 and LPLACE>1 (see data block TRACR), LPLACE is reset to 0 (default) and conventional timestepping is employed.
11. If the number of the summation terms in the Stehfest Laplace transform formulation

NITR<10 or NITR>18 (see data block TRACR), NITR is reset to 18.

12. If the number of the summation terms in the DeHoog Laplace transform formulation NITR<5 or NITR>10 (see data block TRACR), NITR is reset to 6 (default).
13. If the number of the summation terms in the Stehfest Laplace transform formulation NITR is an odd number (see data block TRACR), NITR is reset to min(NITR+1,18).
14. If the maximum number of allowable Newtonian iterations in the tracer equations NOITR$\leq$0 (see data block TRACR), NOITR is reset to 5 (default).
15. If the flag for flow velocity averaging IFFACT<0 or IFFACT>3 (see data block TRACR), IFFACT is reset to 0 (default).
16. If the flag for water saturation averaging ISFACT<0 or ISFACT>3 (see data block TRACR), ISFACT is reset to 0 (default).
17. If the flag for radioactive or reactive decay averaging IDFACT<0 or IDFACT>1 (see data block TRACR), IDFACT is reset to 0 (default).
18. If the maximum Courant number COURAN>1 and the flag for overriding it ICOVRD$\neq$9 (see data block TRACR), COURAN is reset to 1 (default). Note that COURAN=1 is necessary for the explicit solution of the tracer equation(s). In EOS9nT, however, the tracer equation(s) are solved implicitly. Thus COURAN=1 imposes very (and unnecessarily) conservative condition, and can be substantially relaxed with impunity.
19. If the maximum allowed timestep as a fraction of the half-life or the forward reaction constant HLFRAC>0.1 and the flag for overriding it ITOVRD$\neq$9 (see data block TRACR), HLFRAC is reset to 0.1 (default).
20. If the convergence criterion of the Laplace space solutions CRLAPL<1.0E-14 or CRLAPL>1.0E-09 (see data block TRACR), CRLAPL is reset to 1.0E-12 (default). The strict convergence criterion is necessitated by the need for very accurate

Laplace space solutions for accurate time domain solutions.

6.3. Error Messages

Error messages are printed, and the simulations are aborted, in the following cases:

1. If the number of (a) elements, (b) connections, (c) sinks and sources or (d) the work array elements declared in the main program (module `T2CG1.f`) are smaller than the needed values (determined internally by EOS9nT from the input file).
2. If there is a discrepancy between the array dimensions in the main program (module `T2CG1.f`) and in the included module `TRCOMN.f`. This can occur if (a) the numbers of elements, (b) the numbers of connections, (c) the numbers of sink and sources or (d) the numbers of elements in the work arrays differ in the two modules.
3. If the number of tracers `ITRACR` declared in `PARAM` (see card 5.2.1) exceeds the maximum tracer number `NTRCMX` declared in the module `TRCOMN.f`.
4. If the number of tracers `NTRACR` declared in data block `TRACR` exceeds the maximum tracer number `NTRCMX` declared in the module `TRCOMN.f`.
5. If the number of tracers `NTRQ` declared in data block `GENER` (see card 5.7.1) differs from the the number of tracers `NTRACR` declared in data block `TRACR`.
6. If the number of tracers `NTRACR` declared in data block `TRACR` differs from the number of tracers `ITRACR` declared in the data block `PARAM`.
7. If the number of tracers `KTRACR` declared in data block `INCON` differs from the number of tracers `NTRACR` declared in the data block `TRACR`.
8. If the number of rocks/soils for which sorption/filtration data are provided in data block `TRACR` exceeds the number of rocks/soils provided in data block `ROCKS`.
9. If the tracer type `TRTYPE` and the sorption number `NSORPT` in data block `TRACR`

are in conflict. For example, setting TRTYPE='C' and NSORPT<7 causes an error message to be printed and the simulation to be aborted.

10. If the character variable LPTYPE≠'stfs' and LPTYPE≠'hoog', indicating that the numerical inversion method of the Laplace space solution is neither the Stehfest algorithm [*Stehfest*, 1970a;b] nor the De Hoog method [*De Hoog et al.*, 1982].
11. If a tracer is declared a parent or a daughter in a radioactive chain (PCTYPE='P' or PCTYPE='D') and its molecular weight WTMOL=0.
12. If the number of active dimensions NACTDI (determined internally by EOS9nT from the input file) (a) is different from 1, 2 or 3, or (b) exceeds the maximum value NDIM declared in TRCOMN.f.

7. An Example Data File

The input data file TestM is shown below. TestM simulates flow between constant head boundaries, and involves a small grid consisting of 10 active and 2 inactive (boundary) gridblocks. A parent radionuclide `PAR01` is at a constant mass fraction (concentration) at the upstream boundary gridblock. As the parent moves through the domain, it decays into the radionuclide `DTR01`, which in turn decays to the daughter species `DTR02`.

Although the three types of media in ROCKS have the same hydraulic properties, the sorption parameters of the three species in them are different. The porous medium is fully saturated and at steady state. The initial pressure distribution, which produces the time-invariant velocity field, was obtained by running the problem to steady state, starting with constant pressures in the upstream and downstream boundary gridblocks (i.e., `A11 1` and `A1112`, respectively), initial pressures equal to 10^5 Pa everywhere else, and no tracers. The De Hoog method is used to numerically invert the Laplace space solution. The reader is invited to peruse the file for a better understanding of the EOS9nT input requirements.

```
*TestM* 1-D RADIONUCLIDE TRANSPORT
ROCKS----1----*----2----*----3----*----4----*----5----*----6----*----7----*----8
FIN1 2 2650. .30 1.24E-09 1.24E-09 1.24E-09 1.8 1030.
 1.
 1 0. 0. 1. 1.
 1 0.e6 0. 1.
FIN2 2 2650. .30 1.24E-09 1.24E-09 1.24E-09 1.8 1030.
 1.
 1 0. 0. 1. 1.
 1 0.e6 0. 1.
FIN3 2 2650. .30 1.24E-09 1.24E-09 1.24E-09 1.8 1030.
 1.
 1 0. 0. 1. 1.
 1 0.e6 0. 1.
REFCO 1.e5 25.

START----1----*----2----*----3----*----4----*----5----*----6----*----7----*----8
----*----1-MOP: 123456789*123456789*1234----*----5----*----6----*----7----*----8
PARAM----1----*----2----*----3----*----4----*----5----*----6----*----7----*----8
 2 90 902010 0000020000400 04 3
 1.728e7 -1. 2.e4 0.00000
 3.e+03
 1.E-07 1.E0
 1.0e+5
 0.0e-0 0.0e-0 0.0e-0
 0.0e-0 0.0e-0 0.0e-0
 0.0e-0 0.0e-0 0.0e-0
TRACR----1----*----2----*----3----*----4----*----5----*----6----*----7----*----8
 3 10 05 steady1STFS16 1.0e-12
3 3 1 0 0 1.0e-0 1.0e-1
Tc099SOP 1 0 0 0 0 0 0 4.550e-10 6.7218e12 9.900e2 0.0d0 0.0d0
 1 10 0 0.00e-00 0.0e00 0.0e-00 0.00e-00 0.0e00 0.0e-00 0.000e-00
Np238SOP 3 1 0 0 0 0 0 7.123e-10 6.7533e13 2.380e2 0.0d0 0.0d0
 1 10 2 1.00e-03 0.0e00 0.0e-00 0.00e-00 0.0e00 0.0e-00 0.000e-00
 2 4
 3 10 2 4.00e-03 0.0e00 0.0e-00 0.00e-00 0.0e00 0.0e-00 0.000e-00
 5 6
 7 10 2 5.00e-03 0.0e00 0.0e-00 0.00e-00 0.0e00 0.0e-00 0.000e-00
 8 9
Pu239SOP 1 1 0 0 0 0 0 6.080e-10 7.6054e11 2.390e2 0.0d0 0.0d0
 1 10 4 1.00e-01 0.0e00 0.0e-00 0.00e-00 0.0e00 0.0e-00 0.000e-00
 2 3 4 5
ELEME
A11 2 10.7000E+000.1400E+01 0.3500E+000.5000E+00-.5000E+00
A11 3 10.7000E+000.1400E+01 0.1050E+010.5000E+00-.5000E+00
A11 4 20.7000E+000.1400E+01 0.1750E+010.5000E+00-.5000E+00
A11 5 20.7000E+000.1400E+01 0.2450E+010.5000E+00-.5000E+00
A11 6 30.7000E+000.1400E+01 0.3150E+010.5000E+00-.5000E+00
A11 7 30.7000E+000.1400E+01 0.3850E+010.5000E+00-.5000E+00
A11 8 40.7000E+000.1400E+01 0.4550E+010.5000E+00-.5000E+00
A11 9 40.7000E+000.1400E+01 0.5250E+010.5000E+00-.5000E+00
A1110 50.7000E+000.1400E+01 0.5950E+010.5000E+00-.5000E+00
A1111 50.7000E+000.1400E+01 0.6650E+010.5000E+00-.5000E+00
ina
A11 1 10.1000E-050.2000E-05 0.5000E-060.5000E+00-.5000E+00
A1112 10.1000E-050.2000E-05 0.7000E+010.5000E+00-.5000E+00

CONNE
A11 1A11 2 10.5000E-060.3500E+000.1000E+01
A11 2A11 3 10.3500E+000.3500E+000.1000E+01
A11 3A11 4 10.3500E+000.3500E+000.1000E+01
A11 4A11 5 10.3500E+000.3500E+000.1000E+01
A11 5A11 6 10.3500E+000.3500E+000.1000E+01
A11 6A11 7 10.3500E+000.3500E+000.1000E+01
A11 7A11 8 10.3500E+000.3500E+000.1000E+01
A11 8A11 9 10.3500E+000.3500E+000.1000E+01
A11 9A1110 10.3500E+000.3500E+000.1000E+01
```

```
A1110A1111 10.3500E+000.3500E+000.1000E+01
A1111A1112 10.3500E+000.5000E-060.1000E+01

INCON -- INITIAL CONDITIONS FOR 13 ELEMENTS AT TIME 0.172800E+07
A11 2 0.30000000E+00 3
 0.1000016693398E+06
 0.0000000000000E+00 0.0000000000000E+00 0.0000000000000E+00
 0.0000000000000E+00 0.0000000000000E+00 0.0000000000000E+00
 0.0000000000000E+00 0.0000000000000E+00 0.0000000000000E+00
A11 3 0.30000000E+00 3
 0.1000014936198E+06
 0.0000000000000E+00 0.0000000000000E+00 0.0000000000000E+00
 0.0000000000000E+00 0.0000000000000E+00 0.0000000000000E+00
 0.0000000000000E+00 0.0000000000000E+00 0.0000000000000E+00
A11 4 0.30000000E+00 3
 0.1000013178998E+06
 0.0000000000000E+00 0.0000000000000E+00 0.0000000000000E+00
 0.0000000000000E+00 0.0000000000000E+00 0.0000000000000E+00
 0.0000000000000E+00 0.0000000000000E+00 0.0000000000000E+00
A11 5 0.30000000E+00 3
 0.1000011421798E+06
 0.0000000000000E+00 0.0000000000000E+00 0.0000000000000E+00
 0.0000000000000E+00 0.0000000000000E+00 0.0000000000000E+00
 0.0000000000000E+00 0.0000000000000E+00 0.0000000000000E+00
A11 6 0.30000000E+00 3
 0.1000009664598E+06
 0.0000000000000E+00 0.0000000000000E+00 0.0000000000000E+00
 0.0000000000000E+00 0.0000000000000E+00 0.0000000000000E+00
 0.0000000000000E+00 0.0000000000000E+00 0.0000000000000E+00
A11 7 0.30000000E+00 3
 0.1000007907398E+06
 0.0000000000000E+00 0.0000000000000E+00 0.0000000000000E+00
 0.0000000000000E+00 0.0000000000000E+00 0.0000000000000E+00
 0.0000000000000E+00 0.0000000000000E+00 0.0000000000000E+00
A11 8 0.30000000E+00 3
 0.1000006150199E+06
 0.0000000000000E+00 0.0000000000000E+00 0.0000000000000E+00
 0.0000000000000E+00 0.0000000000000E+00 0.0000000000000E+00
 0.0000000000000E+00 0.0000000000000E+00 0.0000000000000E+00
A11 9 0.30000000E+00 3
 0.1000004393000E+06
 0.0000000000000E+00 0.0000000000000E+00 0.0000000000000E+00
 0.0000000000000E+00 0.0000000000000E+00 0.0000000000000E+00
 0.0000000000000E+00 0.0000000000000E+00 0.0000000000000E+00
A1110 0.30000000E+00 3
 0.1000002635800E+06
 0.0000000000000E+00 0.0000000000000E+00 0.0000000000000E+00
 0.0000000000000E+00 0.0000000000000E+00 0.0000000000000E+00
 0.0000000000000E+00 0.0000000000000E+00 0.0000000000000E+00
A1111 0.30000000E+00 3
 0.1000000878601E+06
 0.0000000000000E+00 0.0000000000000E+00 0.0000000000000E+00
 0.0000000000000E+00 0.0000000000000E+00 0.0000000000000E+00
 0.0000000000000E+00 0.0000000000000E+00 0.0000000000000E+00
ina 0 0.30000000E+00 3
 0.1000000000000E+06
 0.0000000000000E+00 0.0000000000000E+00 0.0000000000000E+00
 0.0000000000000E+00 0.0000000000000E+00 0.0000000000000E+00
 0.0000000000000E+00 0.0000000000000E+00 0.0000000000000E+00
A11 1 0.30000000E+00 3
 0.1000017572000E+06
 0.1000000000000E+01 0.1000000000000E+00 0.0000000000000E+00
 0.0000000000000E+00 0.0000000000000E+00 0.0000000000000E+00
 0.0000000000000E+00 0.0000000000000E+00 0.0000000000000E+00
A1112 0.30000000E+00 3
 0.1000000000000E+06
 0.0000000000000E+00 0.0000000000000E+00 0.0000000000000E+00
```

```
 0.0000000000000E+00 0.0000000000000E+00 0.0000000000000E+00
 0.0000000000000E+00 0.0000000000000E+00 0.0000000000000E+00

ENDCY----1----*----2----*----3----*----4----*----5----*----6----*----7----*----8
```

8. Verification of EOS9nT

We tested the performance of EOS9nT against a set of 1-D and 2-D problems with known analytical solutions. When no analytical solutions were availabe (e.g., in the case of solute transport into an unsaturated soil), the EOS9nT results were compared to those from other numerical codes. EOS9nT results were obtained for all three possible treatments of time, i.e., for conventional timestepping (hereafter referred to as the T-solution) and, when possible, for the two Stehfest and De Hoog Laplace space formulations (hereafter refered to as the S and H solutions, respectively).

In all T solutions, the maximum allowable Courant numbers was 0.25, respectively, when timestepping was used. To avoid accuracy problems, in simulations of flow and decay of radioactive tracers with timestepping, the $\Delta t_{t,i}$ was not allowed to exceed $0.05\,T_{1/2}$. Because of the contant flow field and the predictable monotonic decline in the species concentration with x, it was possible to use midpoint weighting in the T solution of these problems. Although this scheme is used in the ensuing example problems because of its higher accuracy, its application is strongly discouraged in fields where the flow and concentration trends are not known a-priori. We strongly urge using a full upstream-

weighting sheme, i.e., using `MOP(11)=0` in `PARAM.1`.

A computer diskette (PC type of format) with all the input files used in our simulations is included as an attachment to this report. Discussions in the ensuing sections will only focus on the performance of EOS9nT, and not on how the various flow and transport properties were computed. For a complete understanding of the problem and the parameters involved in the simulations, the reader is encouraged to study the input files.

8.1. Test Problem 1

Transport of a Non-Sorbing, Non-Radioactive Solute

This problem examines the transport of a single non-sorbing stable isotope ($\lambda = 0$) in a fully saturated, semi-infinite horizontal medium. The groundwater pore velocity is $V = 0.1$ m/day, the dispersion coefficient is $D = 0.1$ m^2/day, and the porosity is ϕ is 0.3. A uniform grid size of $\Delta x = 1$ m is used. Concentration profiles are obtained at $t_1 = 50$ days and $t_2 = 400$ days.

The main purpose of this and all other tests is

(a) to determine the accuracy of the T, S, and H solutions in comparisons

  (i) to analytical results,

  (ii) to each other.

(b) to test the ability of the Laplace transform formulations to produce accurate solutions in a single step.

Two sets of three runs each were conducted for the T, S, and H solutions. For the t_2 profile, an additional test performed in this study evaluated the ability of the De Hoog algorithm to obtain accurate solutions both (a) at the two specified times t_1 and t_2, and (b) at any time t in the interval $[0, t]$ from the solution at t. Thus, the concentration profile at $t = 50$ days was obtained from both the t_1 and the t_2 solutions.

The four (at t_1) and 3 (at t_2) solutions are practically identical, differing in the 3rd decimal place. This test confirms the validity of the 3 solutions, and the ability of the De Hoog method to provide accurate results within the solution period. Figure 3 shows a comparison between the numerical predictions (symbols) and the analytical solutions [*Bear*, 1979]. We observe an excellent agreement between the two sets of solutions. For clarity, the four coinciding solutions are represented by a single symbol.

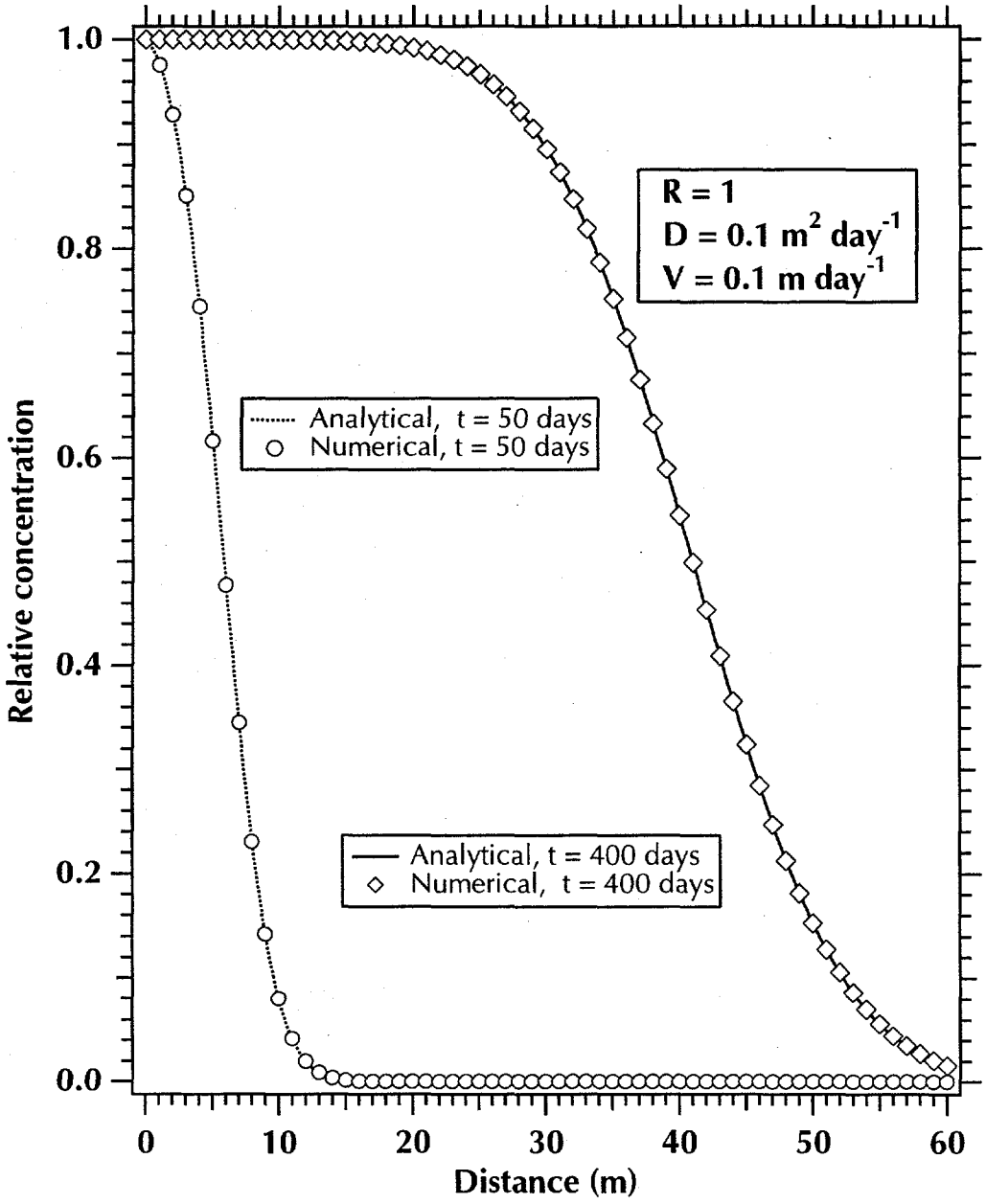

Figure 3. Analytical and numerical solutions at two different times of a non-sorbing, non-radioactive tracer in a semi-infinite column.

8.2. Test Problem 2

Transport of Variably-Sorbing, Non-Radioactive Solute

Test Problem 2 studies the simultaneous transport of five non-interacting non-radioactive ($\lambda_i = 0,\ i = 1, \ldots, 5$) solutes with varying sorption behavior in a fully saturated, semi-infinite horizontal medium. The groundwater pore velocity is $V = 0.1$ m/day, the dispersion coefficient $D = 0.1$ m^2/day, and the porosity is ϕ is 0.3. A uniform grid size of $\Delta x = 1$ m is used. Concentration profiles are sought at $t = 400$ days.

The first species was conservative (i.e., non-sorbing). The retardation factors R of the other four species in the fully saturated medium, defined as

$$R = 1 + \frac{1-\phi}{\phi}\,\rho_s\,K_d \tag{67}$$

were 2, 3, 4 and 5. As in Test Problem 1, a uniform grid size of $\Delta x = 1$ m was used.

In addition to the other goals of the tests (outlined in Section 7.1), this problem evaluated the ability of EOS9nT to treat simultaneously n tracers, with n limited only by the available computer memory.

The T, S and H solutions are practically identical (differring in the 3rd decimal place), and demonstrate the ability of EOS9nT to handle multiple tracers. Figure 4 shows a comparison between the numerical predictions (symbols) and the analytical solutions [*Bear*, 1979] at $t = 400$ days. An excellent agreement between the two sets of solutions is observed. For clarity, the coinciding T, S, and H solutions are represented by a single symbol.

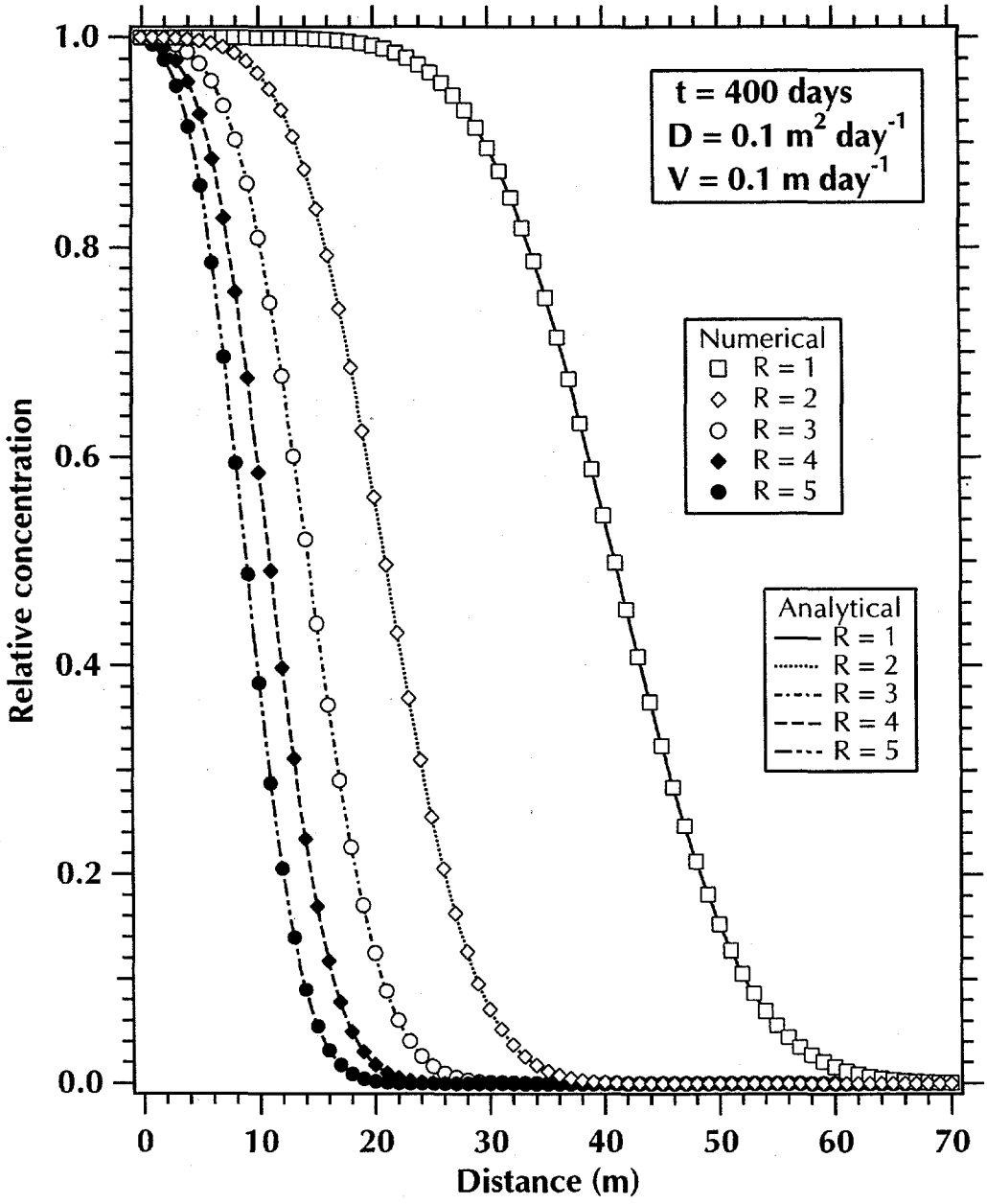

Figure 4. Analytical and numerical solutions of the concentration profile of 5 non-radioactive tracers of variable R in a semi-infinite column.

8.3. Test Problem 3

Transport of a Non-Sorbing Radionuclide in Porous Media

Test Problem 3 describes the transport of a non-sorbing, fast-decaying radionuclide in a fully saturated, semi-infinite horizontal medium. The groundwater pore velocity is $V = 0.2$ m/day, the dispersion coefficient $D = 0.05$ m^2/day, and the porosity of the medium ϕ is 0.3. The half-life of the radionuclide is $T_{1/2} = 69.32$ days. As in Test Problems 1 and 2, a uniform grid size of $\Delta x = 1$ m is used. Concentration profiles are obtained at $t_1 = 50$ days and $t_2 = 200$ days.

Three solutions (T, S, and H) were obtained for t_2. The same solutions were also obtained for t_1, but, as in Test Problem 1, the t_1 distribution was obtained from the t_2 H solution. In Figure 5, the numerical solutions and the analytical solution of *Bear* [1979] coincide. As before, for clarity, the coinciding T, S, and H solutions are represented by a single symbol.

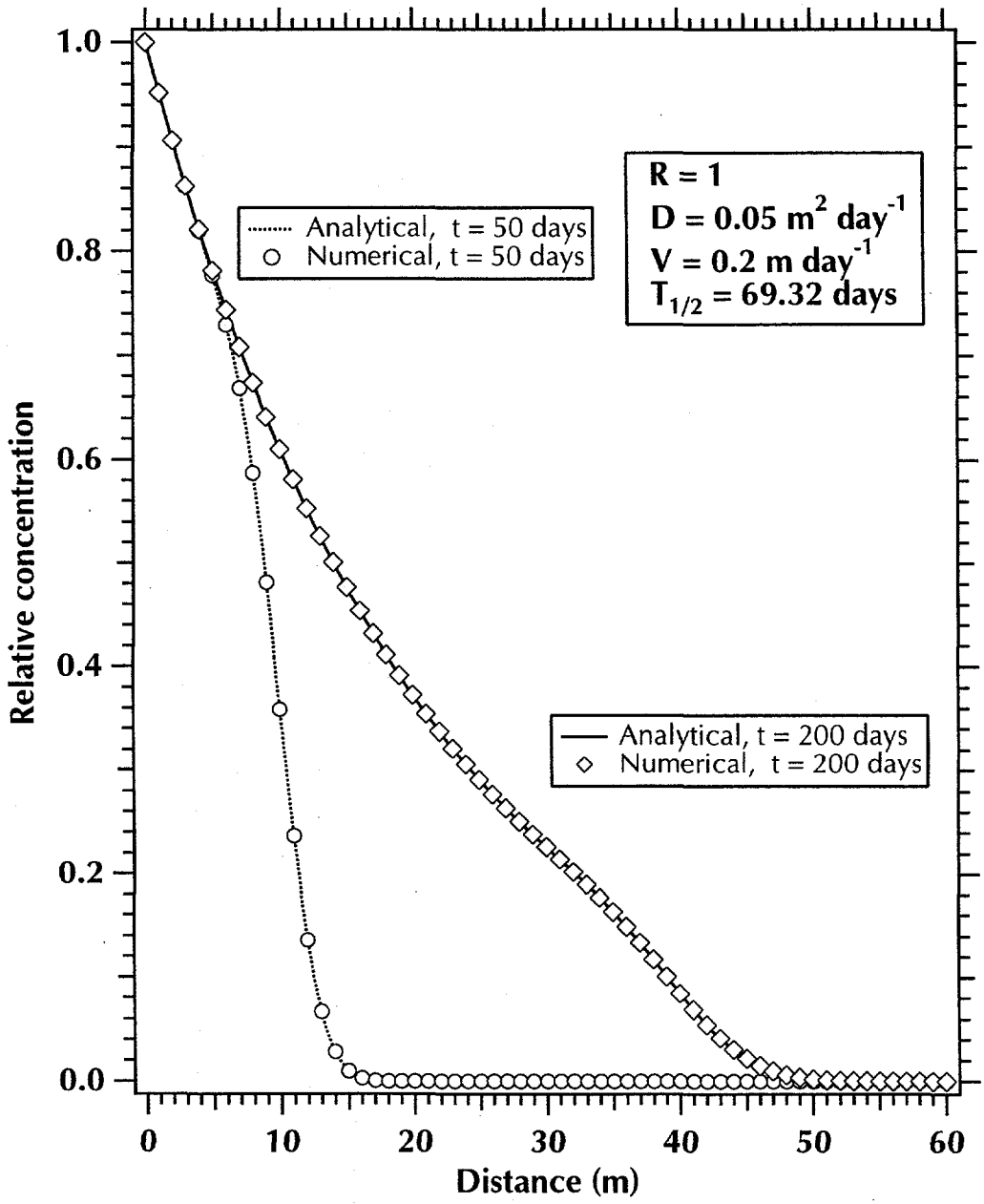

Figure 5. Analytical and numerical solutions of the concentration distribution of a non-sorbing radioactive tracers at two different times.

8.4. Test Problem 4

Transport of Variably-Sorbing Radioactive Tracers in Porous Media

The transport of three non-interacting radioactive tracers with varying decay and sorption behavior are studied in Test Problem 4. The three species are transported by groundwater flowing at a pore velocity $V = 0.1$ m/day in a fully saturated, semi-infinite horizontal formation. The half-live of two of the radionuclides is $T_{1/2} = 69.32$, and of the third is $T_{1/2} = 693.2$. The retardation factors R are between 1 and 2. The dispersion coefficient and the porosity are as in Test Problem 3. A uniform grid size of $\Delta x = 1$ m is used. Concentration profiles are obtained at $t_2 = 200$ days.

The symbols in Figure 6 denote the practically identical T, S, and H solutions, and the coinciding analytical solution of *Bear* [1979]. These results demonstrate that all solution options in EOS9nT can handle accurately multiple species with different transport and decay properties.

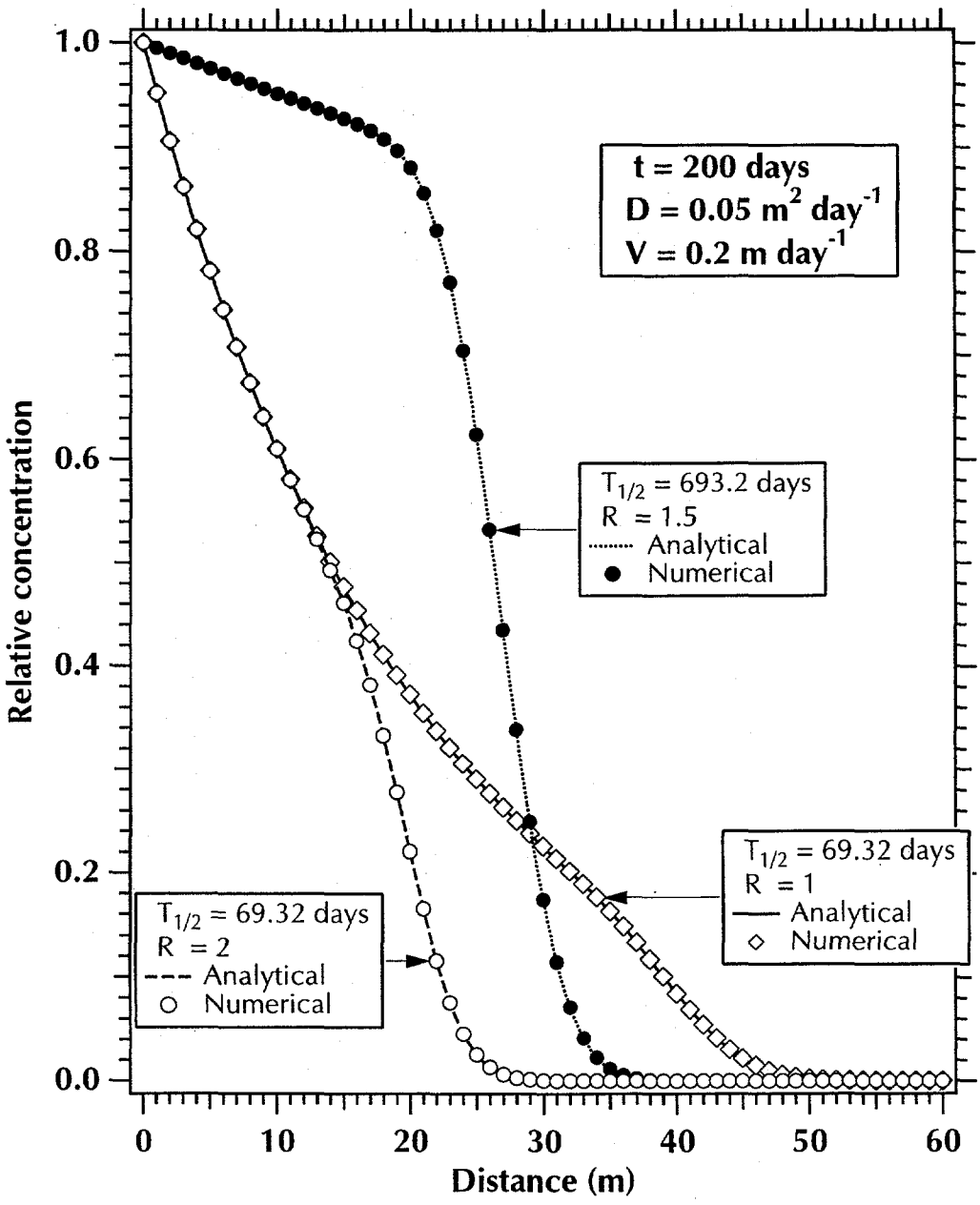

Figure 6. Analytical and numerical solutions of the concentration profiles of three radioactive tracers with variable sorption behavior at $t = 200$ days.

8.5. Test Problem 5

Transport of Radioactive Parents and Daughters in Porous Media

Test Problem 5 describes the migration behavior of the decay chain $^{234}U \rightarrow {}^{230}Th \rightarrow {}^{226}Ra$ in a saturated porous medium. The most important species is ^{226}Ra because it is very mobile in geologic media and has high biohazard potential. An extensive analysis of the problem can be found in *Harada et al.* [1980].

The half-lives of ^{234}U, ^{230}Th, and ^{226}Ra are 2.44×10^5, 7.7×10^4 and 1.60×10^3 years, respectively. All three species are strong sorbers, with retardation coefficients $K_d = 10^4$ for ^{234}U, 4×10^4 for ^{230}Th and 5×10^2 for ^{226}Ra. In this problem, the other transport parameters are those used by *Harada et al.* [1980]: the groundwater velocity is $V = 100$ m/yr, and the the dispersion coefficient $D = 2.74$ m^2/day

At $t = 5 \times 10^5$ years, the agreement in Figure 7 between the analytical solution and the EOS9nT solution with the DeHoog formulation (denoted as EOS9nT-H in Figure 7) for all three species is excellent. The same is not observed when the Stehfest formulation is used in EOS9nT (denoted as EOS9nT-S). Figure 8 shows that the agreement between the analytical solution and the EOS9nT-S predictions of ^{234}U distribution is excellent up to a distance of 1000 m, but exhibits an oscillatory behavior past that point. The comparison of the ^{230}Th and ^{226}Ra curves to the analytical solutions show very large deviations.

The main reason for the deterioration in the performance of EOST9nT-S is inaccuracies introduced to the solutions via two ways. The first is the very large observation time, which causes roundoff errors in the computations. The second is that the Stehfest algorithm ignores the imaginary part of the Laplace parameter s, which can cause serious problems. These errors are very significant because their effect is amplified as the Laplace space solutions are inverted, and are attested to by the very erroneous solutions for ^{230}Th and ^{226}Ra. This is

the reason why the convergence criterion for the PCG tracer solutions in the Laplace space is 10^{-12}, but only 10^{-6} in regular timestepping.

In our experience, the Stehfest algorithm is very powerful, simple and fast for the simulation of any solute or colloid problem when $t > 1000$ years, but its performance can deteriorate fast past that point. This deterioration is not problem specific, but is numeric in nature and due to the reasons dicussed above. For $t \leq 1000$ years, the Stehfest formulation yields accurate predictions of parent transport, but it is inadvisable to track daughter transport because the small errors in the solution for the parent are sufficient to contaminate the solution for the daughters. On the other hand, the De Hoog formulation is free of these problems for parents or daughters, and yields accurate solutions for any time we have tried.

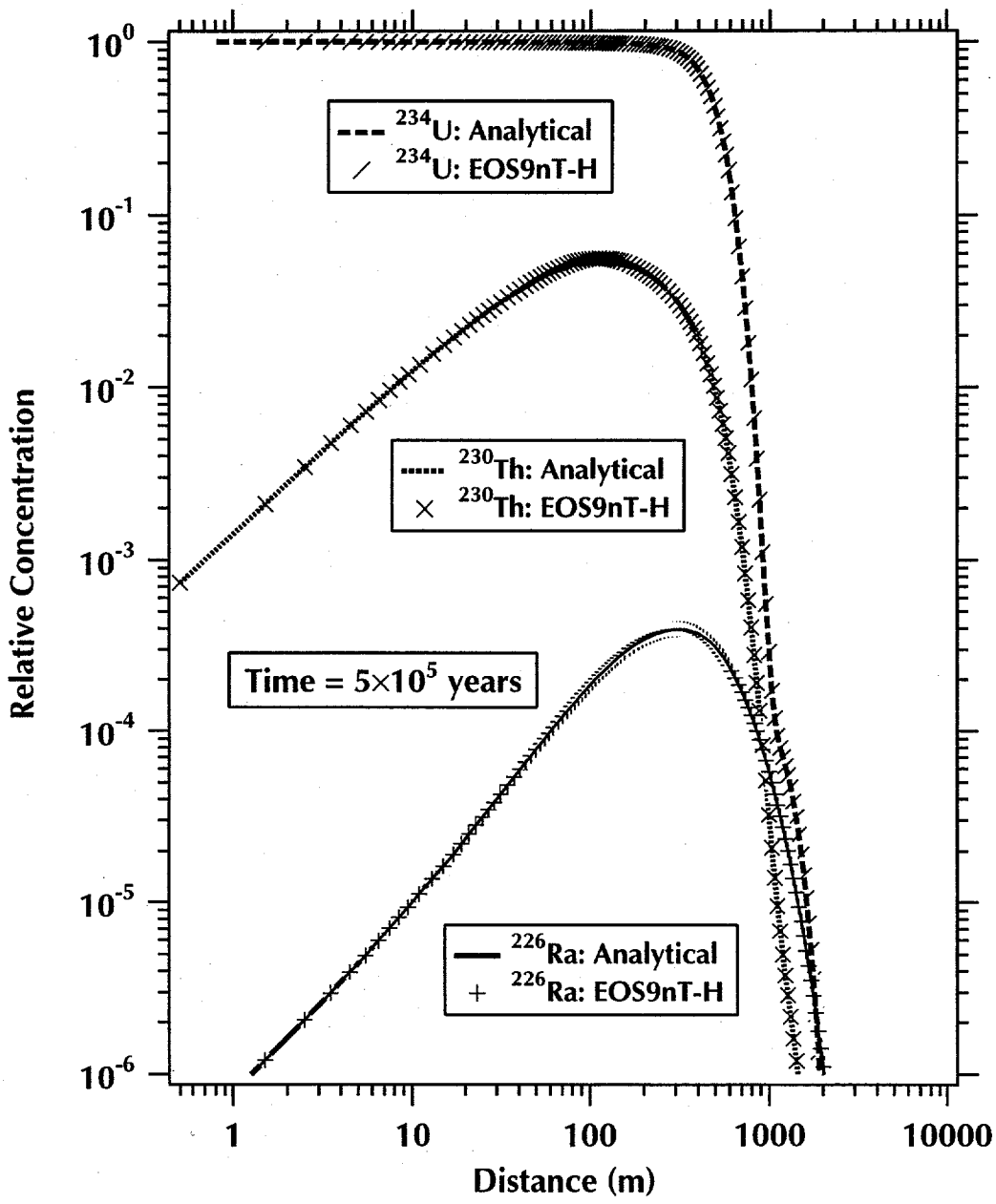

Figure 7. Comparison of analytical predictions of the concentration profiles of the species in the decay chain $^{234}U \rightarrow {}^{230}Th \rightarrow {}^{226}Ra$ to the EOS9nT solution with the De Hoog method for Laplace formulation.

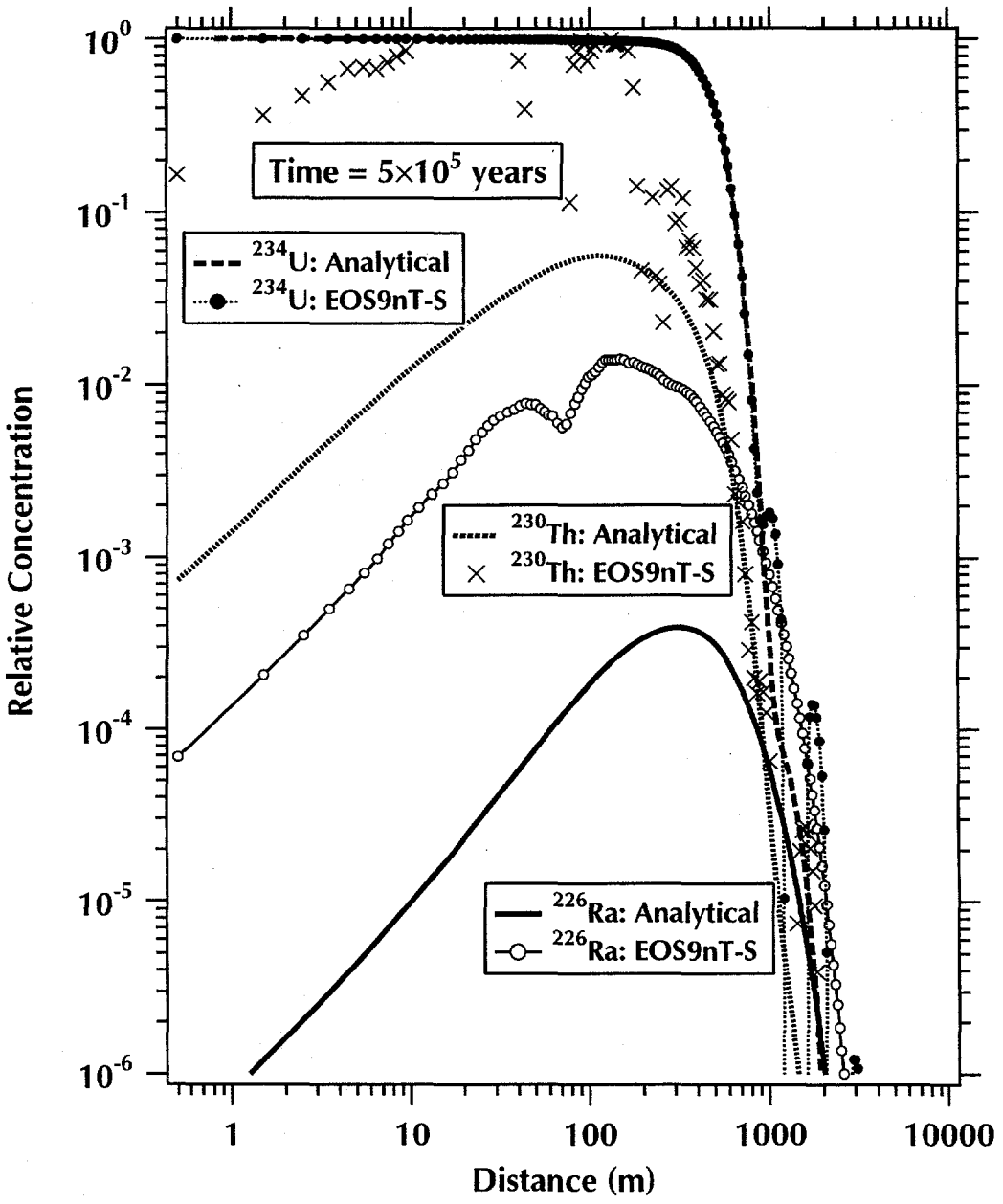

Figure 8. Comparison of analytical predictions of the concentration profiles of the species in the decay chain $^{234}U \rightarrow {}^{230}Th \rightarrow {}^{226}Ra$ to the EOS9nT solution with the Stehfest algorithm for Laplace formulation.

8.6. Test Problem 6

Transport of Radioactive Species in Fractured Media

The transport of radionuclides in fractured media in Test Problem 6 involves a single fracture and a matrix block of finite thickness. The analytical 2-D solution to this problem was developed by *Sudicky and Frind* [1982], and assumes only diffusion but no advection through the matrix.

The parameters used in Test Problem 6 are those of the large fracture-spacing case in the *Sudicky and Frind* [1982] paper. The fracture width $2b = 100$ μm, the matrix porosity $\phi = 0.01$, the matrix tortuosity $\tau = 0.1$, the fracture longitudinal dispersivity $a_L = 0.1$ m, and the diffusion coefficient $D = 1.6 \times 10^{-9}$ m^2/s. The species is a non-sorbing radionuclide ($R = 1$) with $T_{1/2} = 12.35$ yrs. The water velocity is $V = 0.1$ m/s, and the matrix block width is $2B = 0.5$ m.

Three different grids 2-D grids in (x, z) were used for the EOS9nT simulations, with increasing finer discretization in the matrix block. The discretization of the coarse grid was 2×320 in (x, z), with the fracture and the matrix each occupying a single gridblock at any z level. The discretization of the medium and the fine grids were 5×320 and 12×320 in (x, z), respectively.

Figures 9 through 12 show the concentration distribution in the fractures at $t = 100$, $1,000$, $10,000$ and $100,000$ days. All 3 EOS9nT solutions (i.e., T, S and H) for all discretizations are represented in the figures, as their results were extremely close. The comparison to the analytical solution shows that the coarse grid yields inaccurate results, which tend to indicate an early breakthrough. The medium and fine grids, however, return very accurate solutions which are very close to each other.

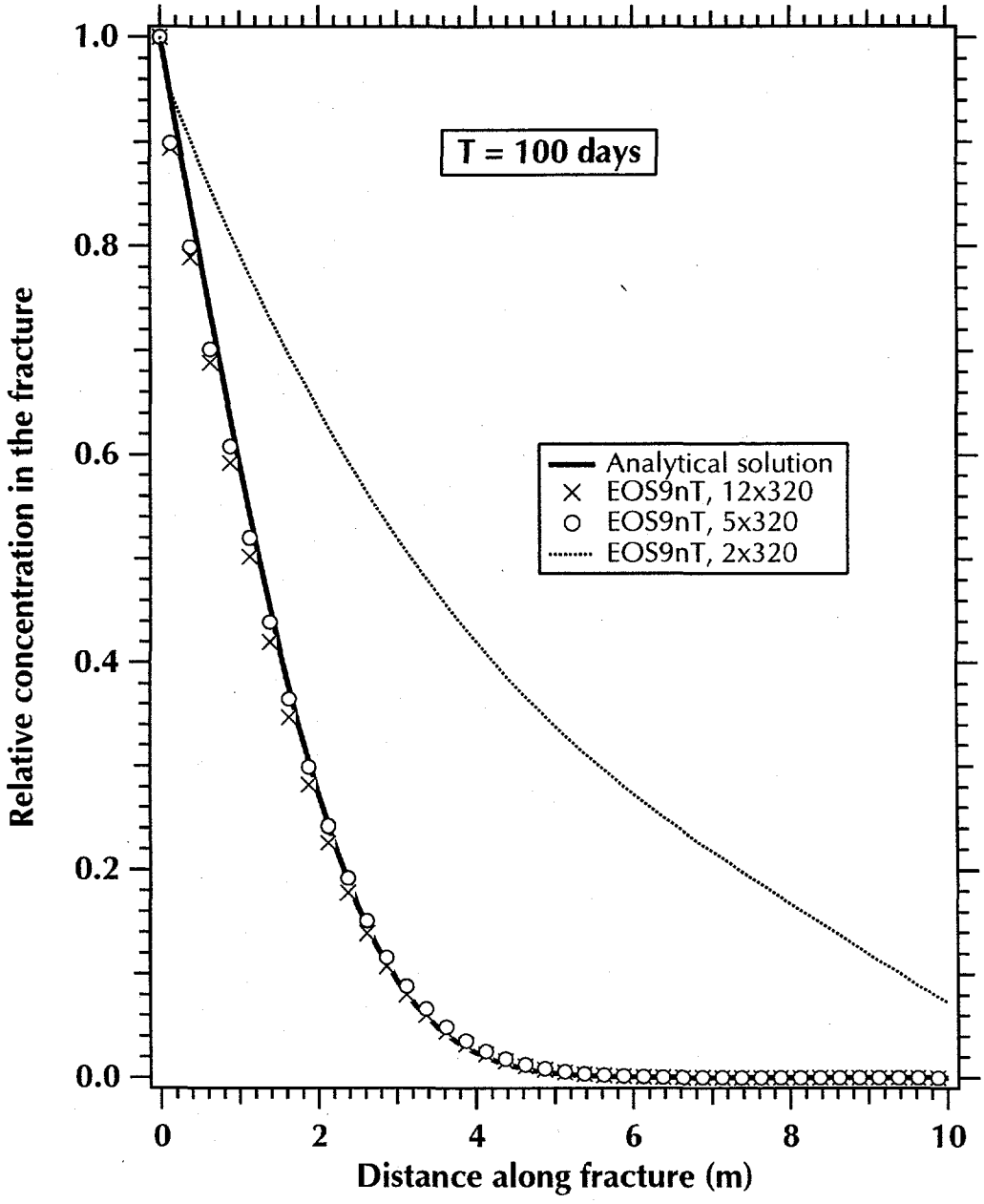

Figure 9. Analytical and numerical solutions of the concentration distribution in a fracture for three different grids at $t = 100$ days. The error caused by the coarse discretization accuracy is significant. The solutions for a medium and coarse grid are indistinguishable.

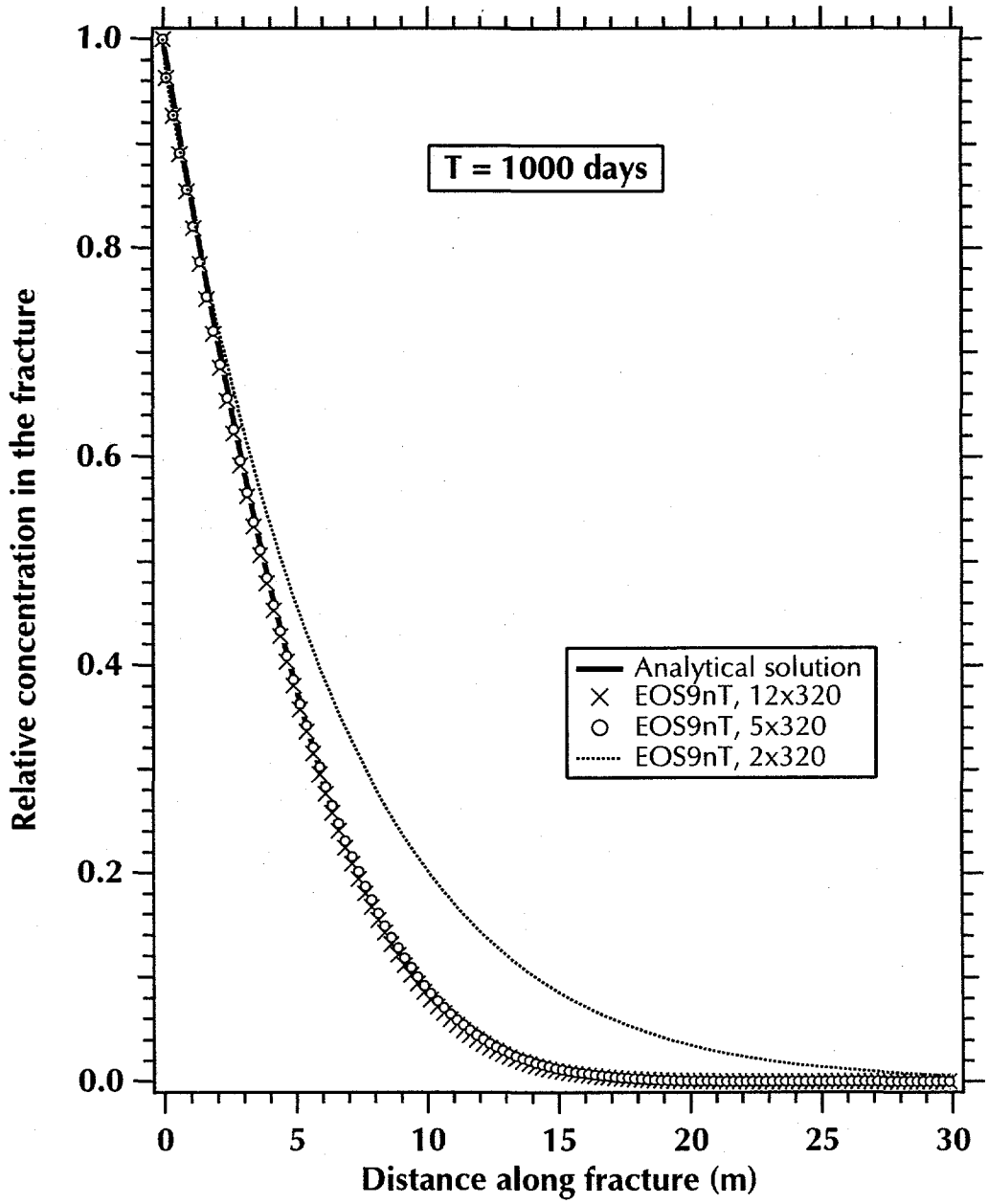

Figure 10. Fracture concentration distribution at $t = 1000$ days. The deviations between the numerical solution for the coarse grid, and the ones for the medium and the fine grids, are becomming smaller.

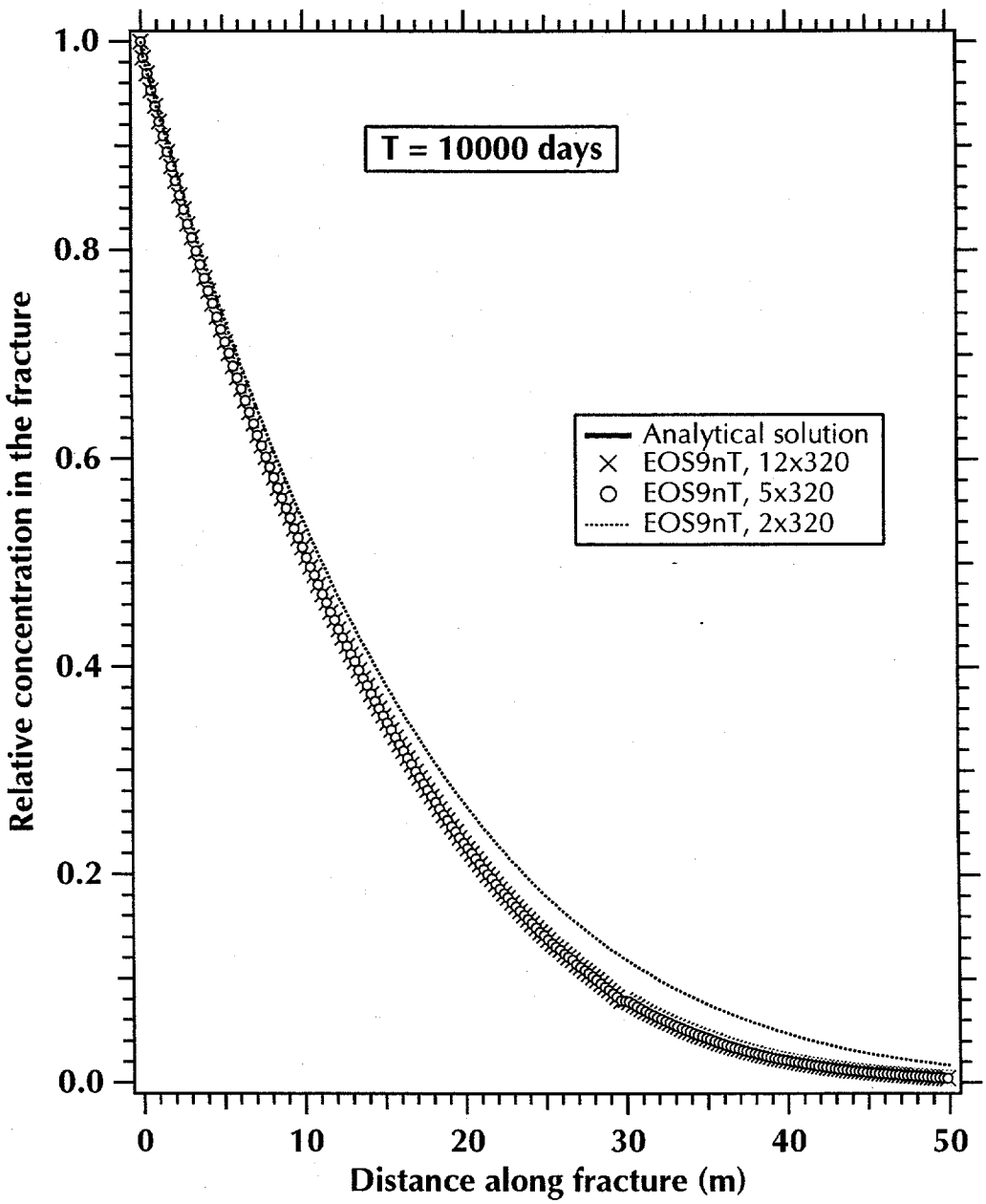

Figure 11. At $t = 10,000$ days, the EOS9nT solutions with medium and fine grids coincide with the analytical. The deviation of the solution for the coarse grid is still measurable, although much smaller that at eariler times.

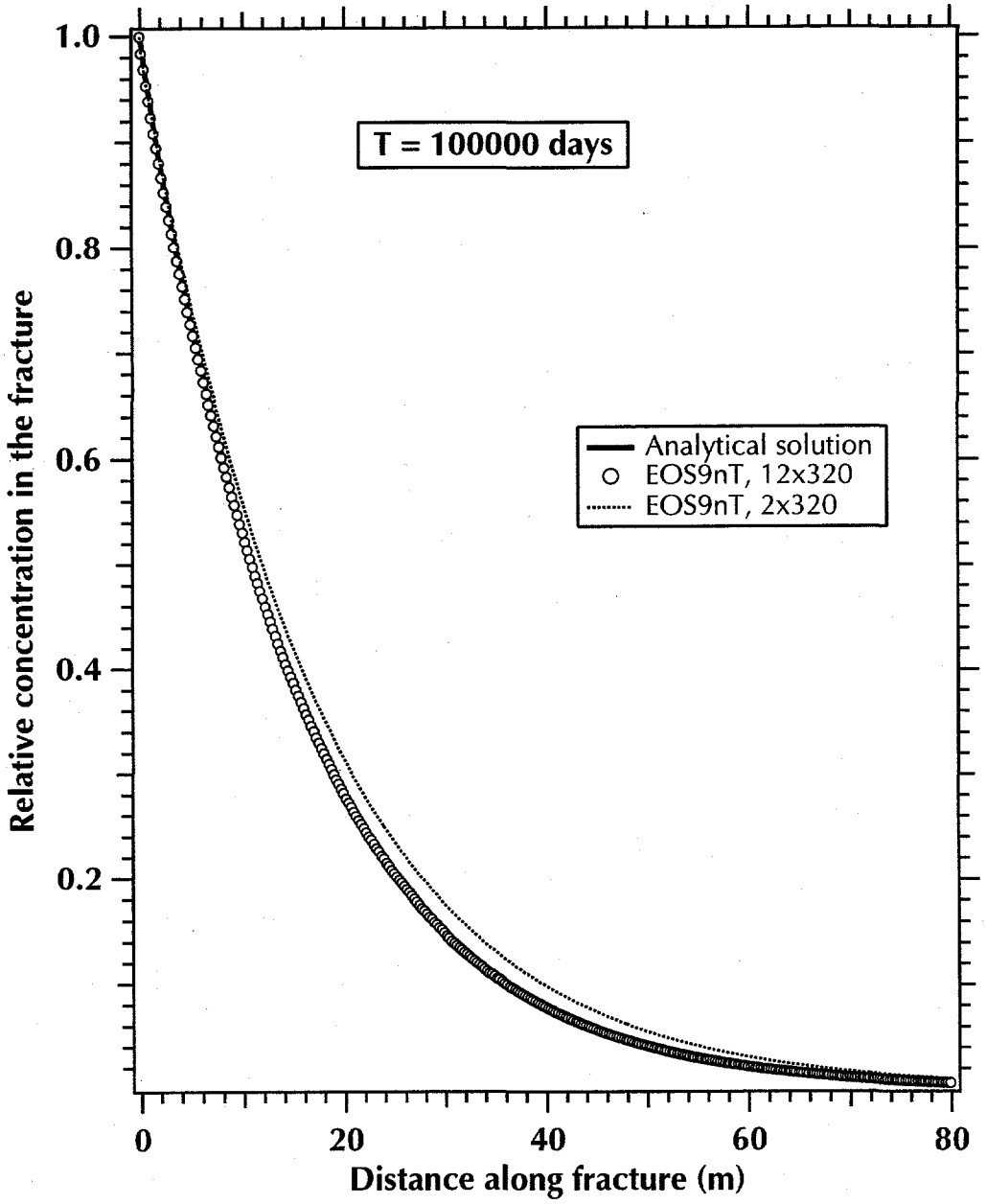

Figure 12. At $t = 100,000$ days, the coarse grid solution converges with all the other solutions.

8.7. Test Problem 7

Colloid Transport in Porous Media

Test Problem 7 involves the transport of three non-sorbing, non-radioactive colloids in a saturated semi-infinite horizontal column. In most colloid studies it is assumed that filtration has an effect on both the porosity and permeability of the porous medium. Under the conditions and assumptions discussed in Section 2.1, this is not the case here, and colloid transport is governed by the kinetic equation (13)[*Corapcioglu*, 1997].

The only analytical solution of the flow and filtration of colloids without affecting the hydraulic properties of the medium was developed by *Dieulin* [1982], and considers only clogging without any mechanism for declogging.

The other parameters were $V = 2$ m/day, $D = 1$ m^2/day, and $\phi = 0.3$. By selecting appropriate coefficients in equations (22) and (23), the filter coefficient ϵ of the three colloids were 30 m^{-1}, 100 m^{-1}, and 3000 m^{-1}, respectively. A uniform grid size of $\Delta x = 0.01$ m was used. At $t = 7600$ s, the analytical and the numerical solutions of EOS9nT (T, S and H) in Figure 13 practically coincide.

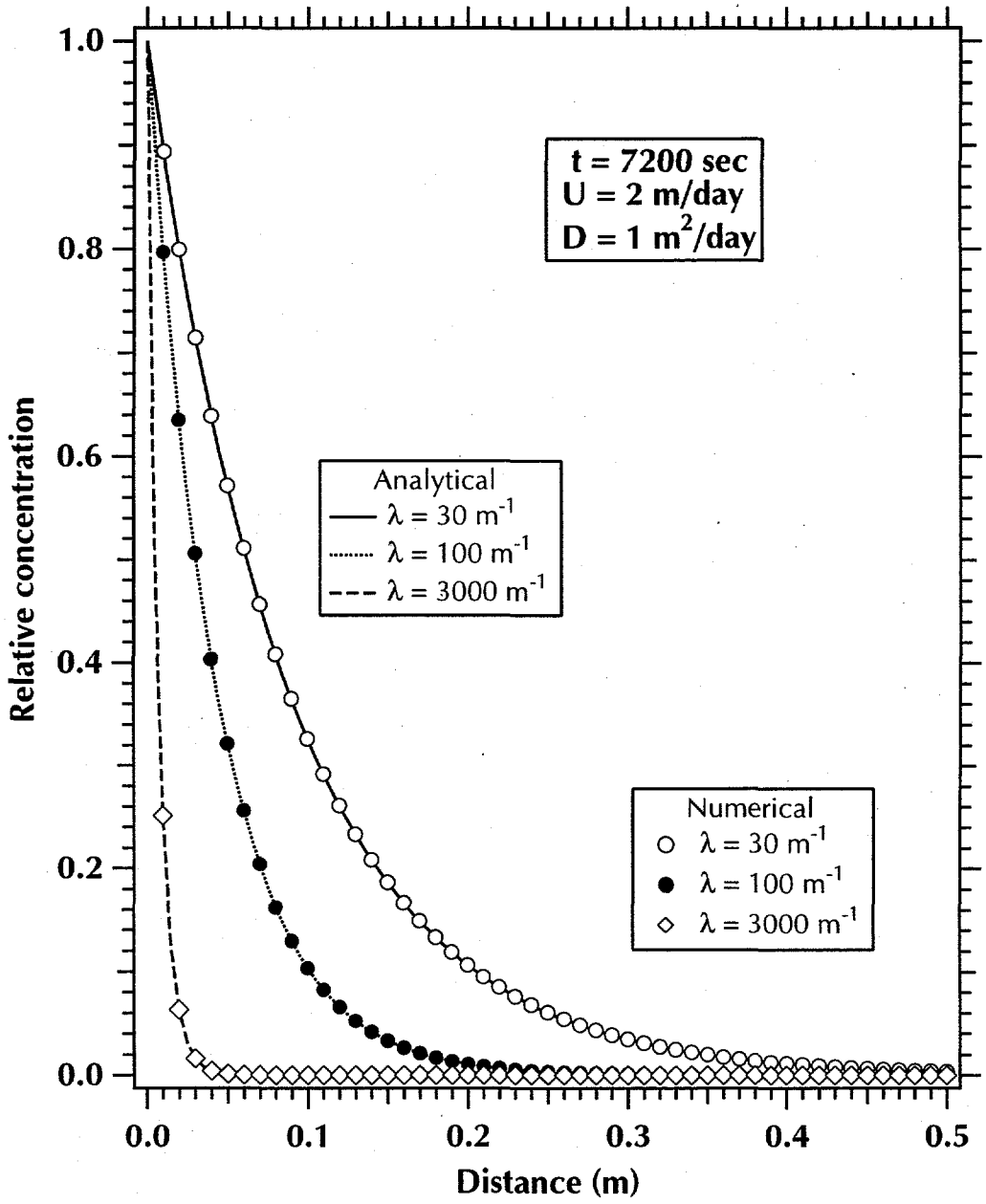

Figure 13. Analytical and numerical predictions of the concentrations of three non-sorbing, non-radioactive colloids.

8.8. Test Problem 8

2- and 3-D Transport of Non-Sorbing Non-radioactive Species

The system simulated in Test Problem 8 is shown in Figure 14, and involves 2-D transport with hydrodynamic dispersion. An analytical solution to this problem was developed by *Cleary and Ungs* [1978], and a computer FORTRAN program to solve it was provided by *Javandel et al.* [1984].

Two sets of runs were made. The first set involves the discretization of the 2-D domain in Figure 14, while the second set is a pseudo-3-D system obtained by discretizing a finite thickness in the y direction and assigning everywhere the properties of the 2-D system. Because of symmetry, the two sets of solutions must be identical.

The runs were made with $V = 0.5$ m/day and $A = 50$ m^2. The longitudinal and transverse components of dispersivity, D_L and D_T, are 5 m^2/day and 0.5 m^2/day, respectively, and the species was assumed conservative ($R = 1$). The results at $t = 365$ days and along the axes at $y = 0$ and $y = 40$ m are shown in Figure 15, where the symbols for the numerical solutions represent a set of 6 near identical values: a set of 3 solutions (T, S and H) for each of the 2-D and the pseudo-3-D system.

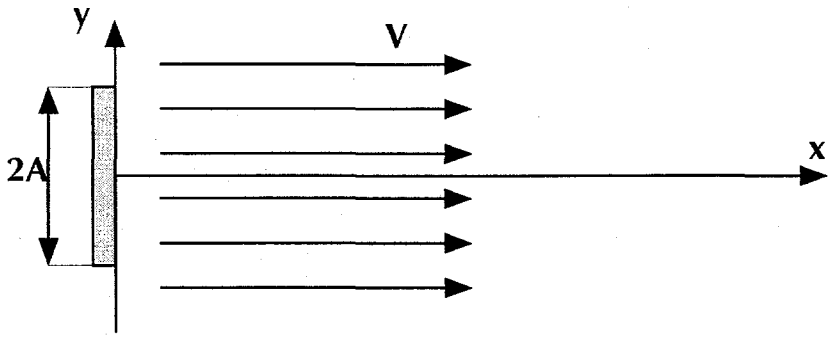

Figure 14. A diagram showing the 2-D simulation domain in Test Problem 8 *Javandel et al.* [1984].

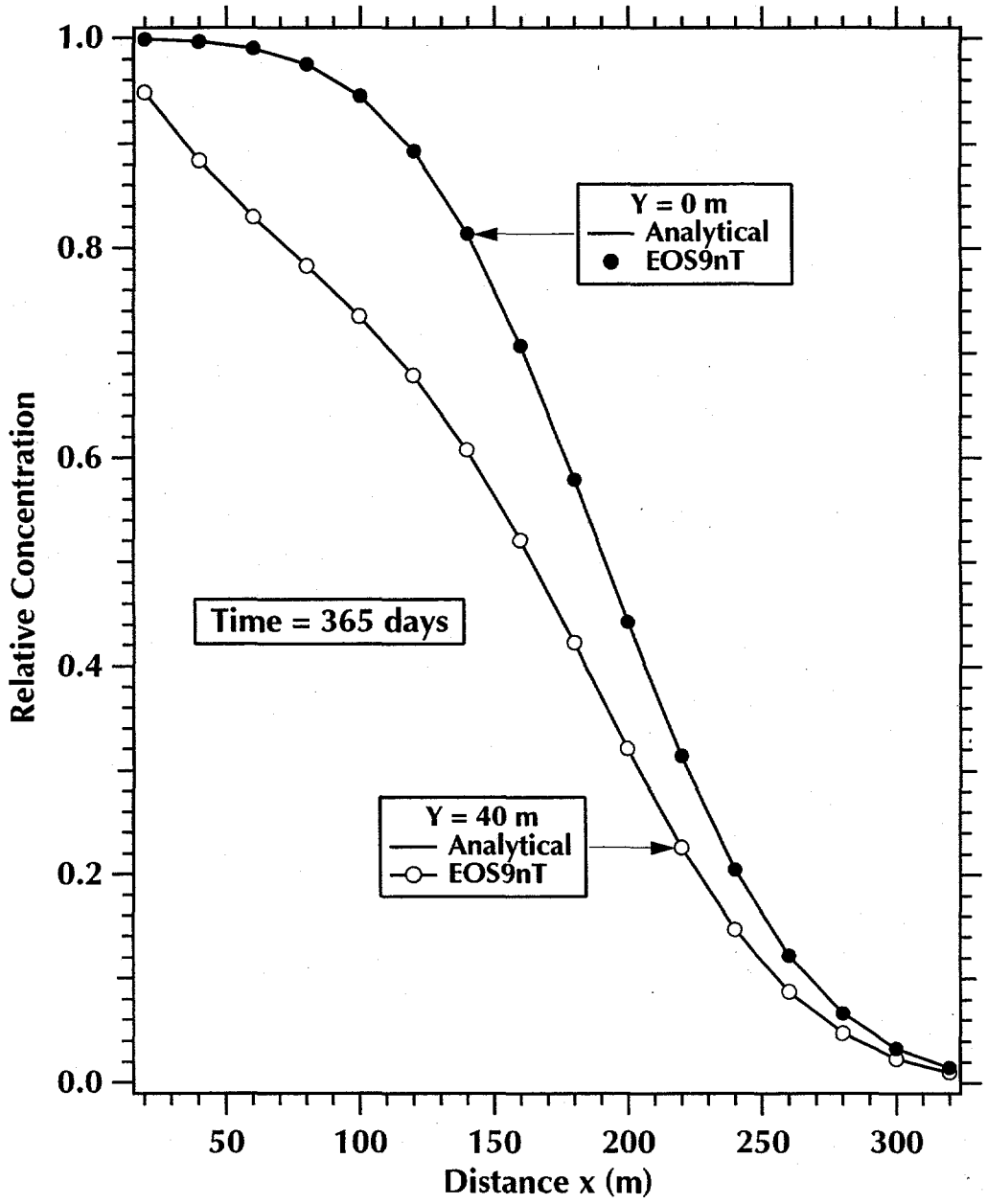

Figure 15. Analytical and EOS9nT concentration distributions for the problem of Figure 14 along the axes at $y = 0$ m and $y = 40$ m.

8.9. Test Problem 9

Flow and Transport into an Unsaturated Column

Test Problem 9 is the horizontal infiltration problem originally solved by *Philip* [1955]. A semi-infinite horizontal tube filled with a homogeneous soil is partially saturated with water. The soil porosity is $\phi = 0.45$, and the initial moisture content is $\theta = 0.2$, corresponding to a liquid saturation of $S_w = \theta/\phi = 0.44$. The liquid saturation at the $x = 0$ boundary is held constant at $S_w = 1$ for $t > 0$. Due to a capillary pressure differential, water infiltrates into the horizontal system. Air is considered a passive phase, and its effects are neglected.

The problem was augmented by adding two tracers to the water at the $x = 0$ boundary. The mass fractions of the first and second tracers were $X_1 = 10^{-3}$ and $X_2 = 10^{-4}$, respectively. Note that, because of linearity, any value can be used for X, and $X = 1$ is very convenient. The first tracer was non-decaying, and had a $R = 2$. The second tracer was non-sorbing ($R = 1$) and had a $T_{1/2} = 1$ day.

Because of the unsaturated conditions and the nonlinearity of the problem, the Laplace transform formulations cannot be used, and only the timestepping solution is employed. Using the EOS9nT module and the EOS7R module [*Oldenburg and Pruess*, 1995], solutions were obtained at $t = 0.01$ day, $t = 0.06$ days, and $t = 0.11$ days. A uniform grid size of $\Delta x = 0.002$ m was used.

In Figure 16 we compare the numerical (EOS9nT and EOS7R) and analytical solutions of saturation *Philip* [1955] at the three observation times. The two sets of solutions are in excellent agreement. Figures 17 and 18 show the EOS9nT and EOS7R solutions of the concentration distributions of the two tracers at the same times. The EOS9nT and EOS7R solutions were identical in all cases.

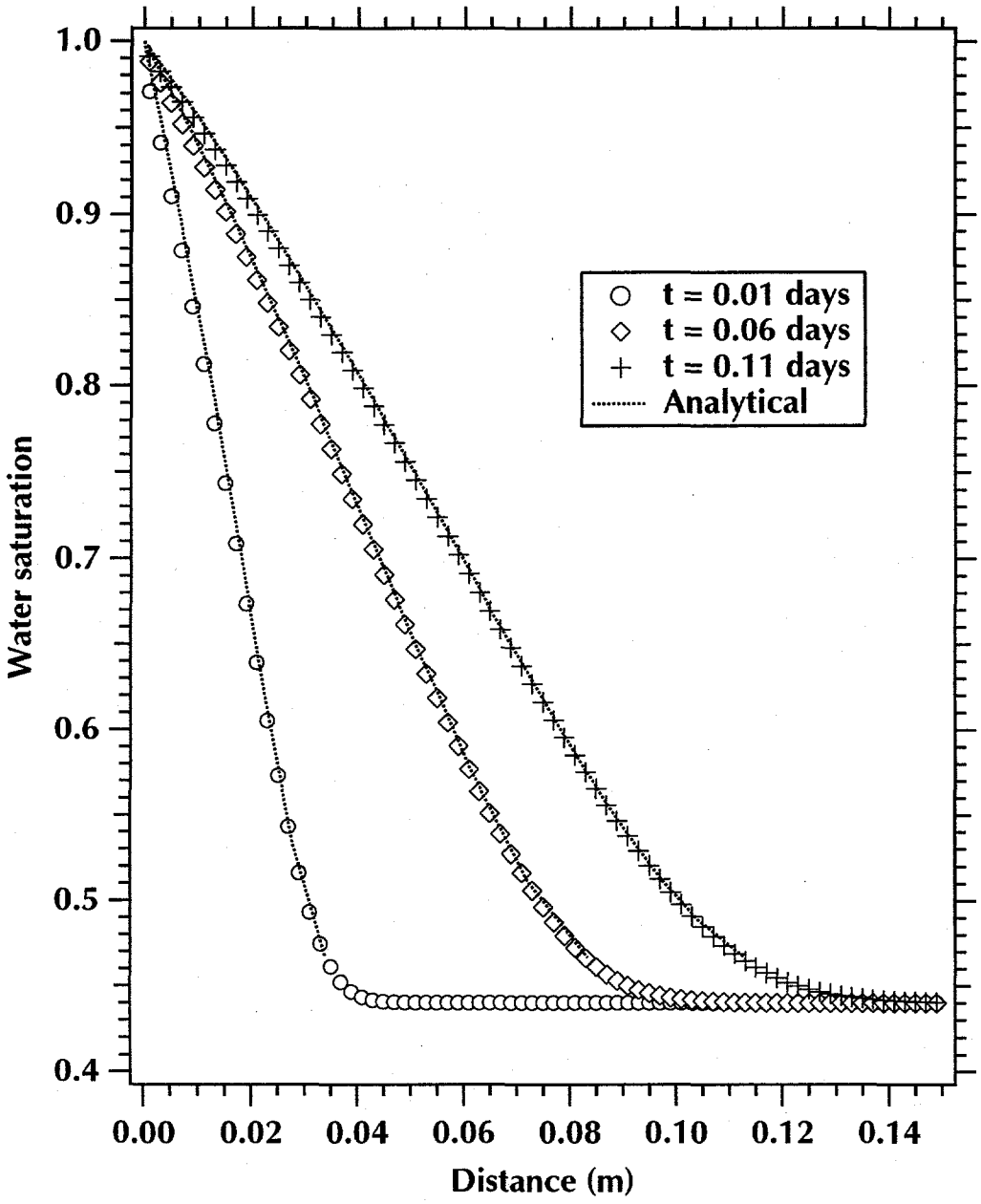

Figure 16. Analytical and numerical solutions of the water saturation distribution in Test Problem 9.

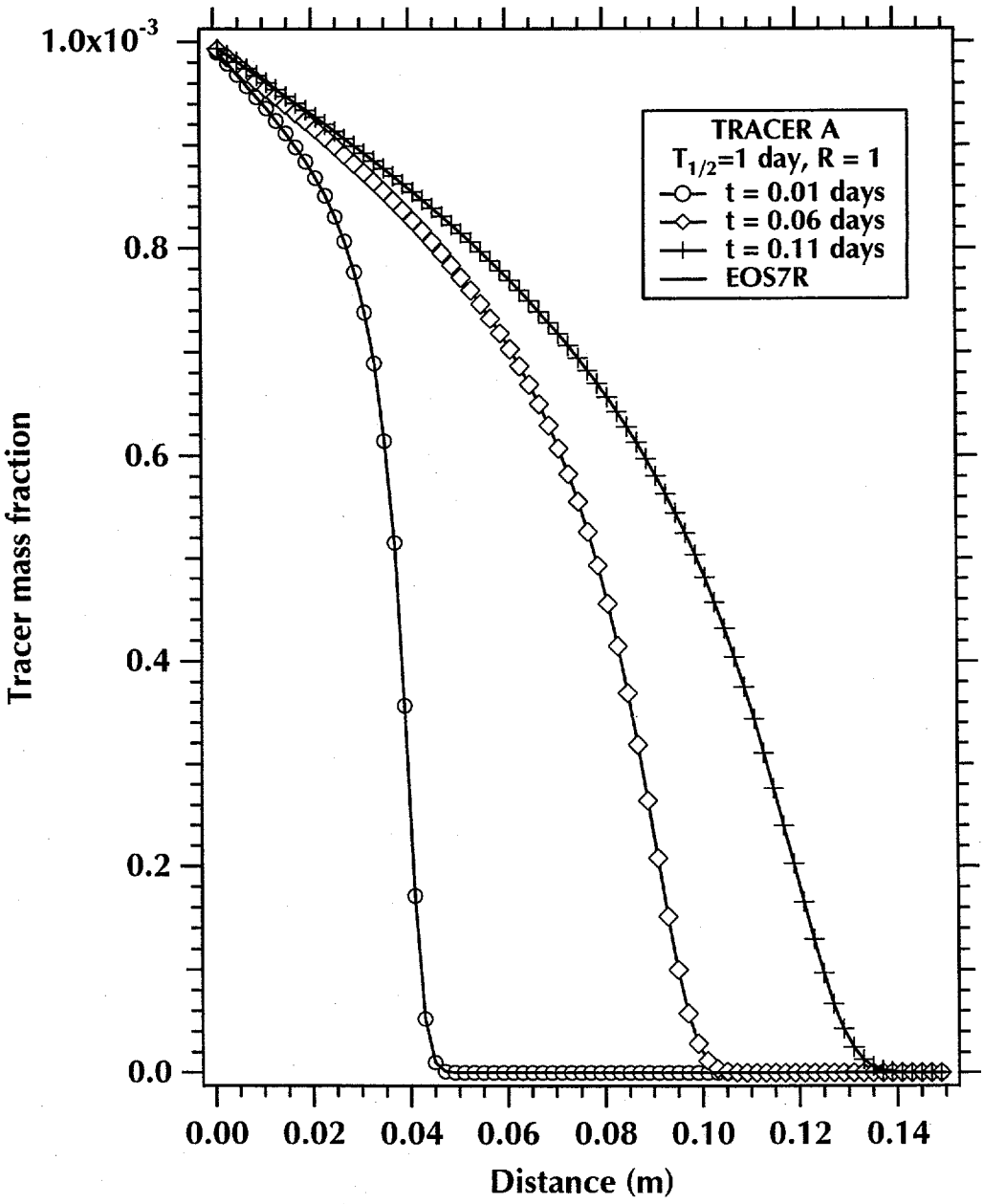

Figure 17. Numerically predicted concentration of a sorbing non-decaying tracer using the EOS9nT and the EOS7R modules.

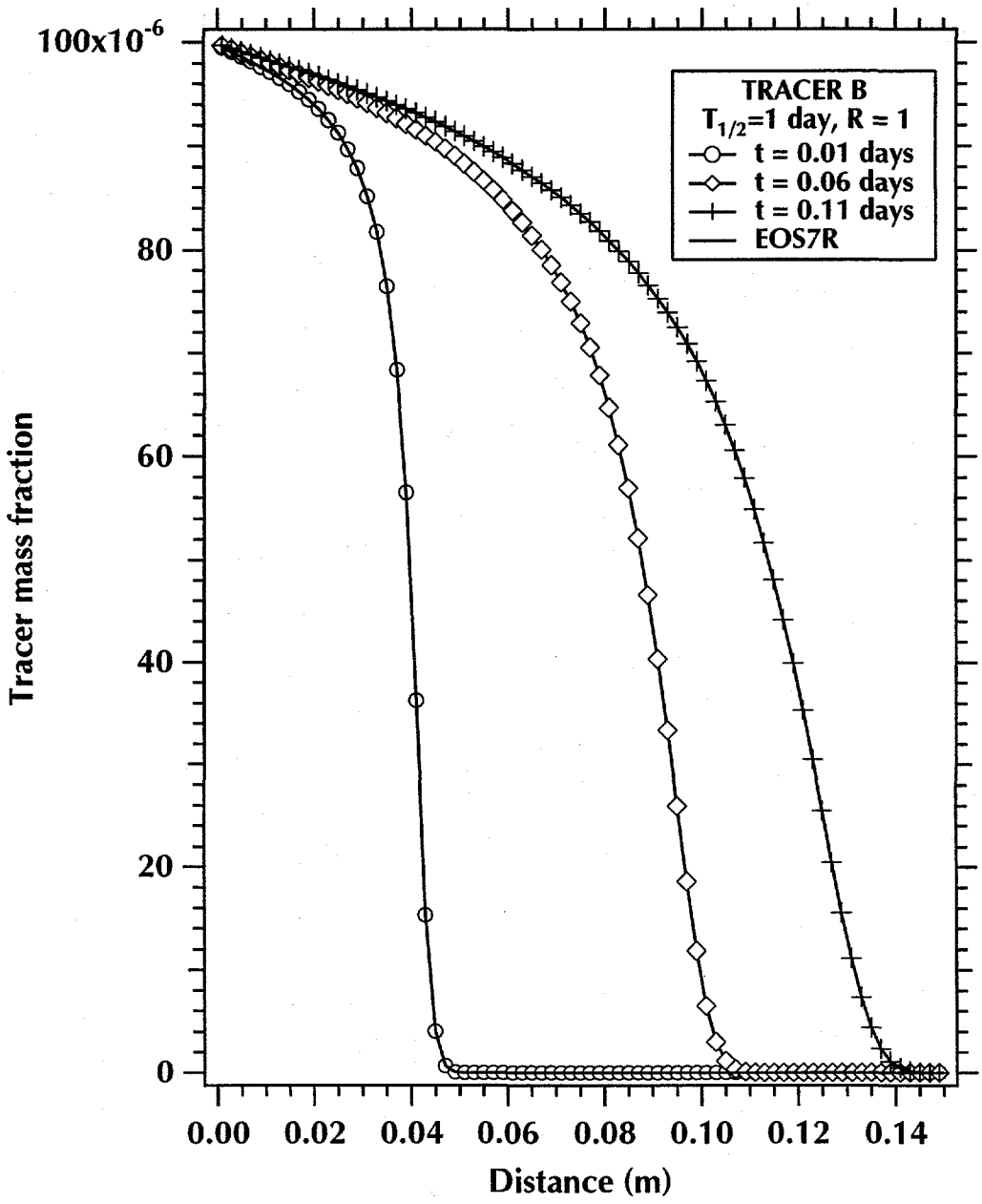

Figure 18. Numerically predicted concentration of a non-sorbing radioactive tracer using the EOS9nT and the EOS7R modules.

8.10. Test Problem 10

Diffusion with Kinetic Sorption in a Diffusion Cell

Test Problem 10 addresses the issue of diffusion and sorption under the conditions of diffusion cell experiments, which involve finite liquid volumes and temporally variable concentrations in the upstream and downstream reservoirs. The semianalytical solutions to this problem were developed by *Moridis* [1999].

The diffusion cell is assumed to have upstream and downstream reservoir volumes $V_U = V_D = 2$ L, and a cross sectional area of the rock sample $A = 10$ cm^2. The sample is 1 cm across, has a porosity of $\phi = 0.35$, and a diffusion coefficient $D_0 = 10^{-10}$ m^2/s.

Figure 19 shows the comparison of the three EOS9nT solutions (T, S and H) of the relative concentrations C_{RU} and C_{RD} of the upstream and downstream reservoirs, respectively, to the semi-analytical solution for a kinetic sorption with $k_\ell = 10^{-2}\ s^{-1}$ and a $K_d = 5.1568 \times 10^{-2}$ m^3 kg^{-1}. Note that C_{RU} and C_{RD} are computed with respect to the initial concentration in the upstream reservoir. When at equilibrium, this K_d corresponds to an R^* of 250. The three solutions practically coincide.

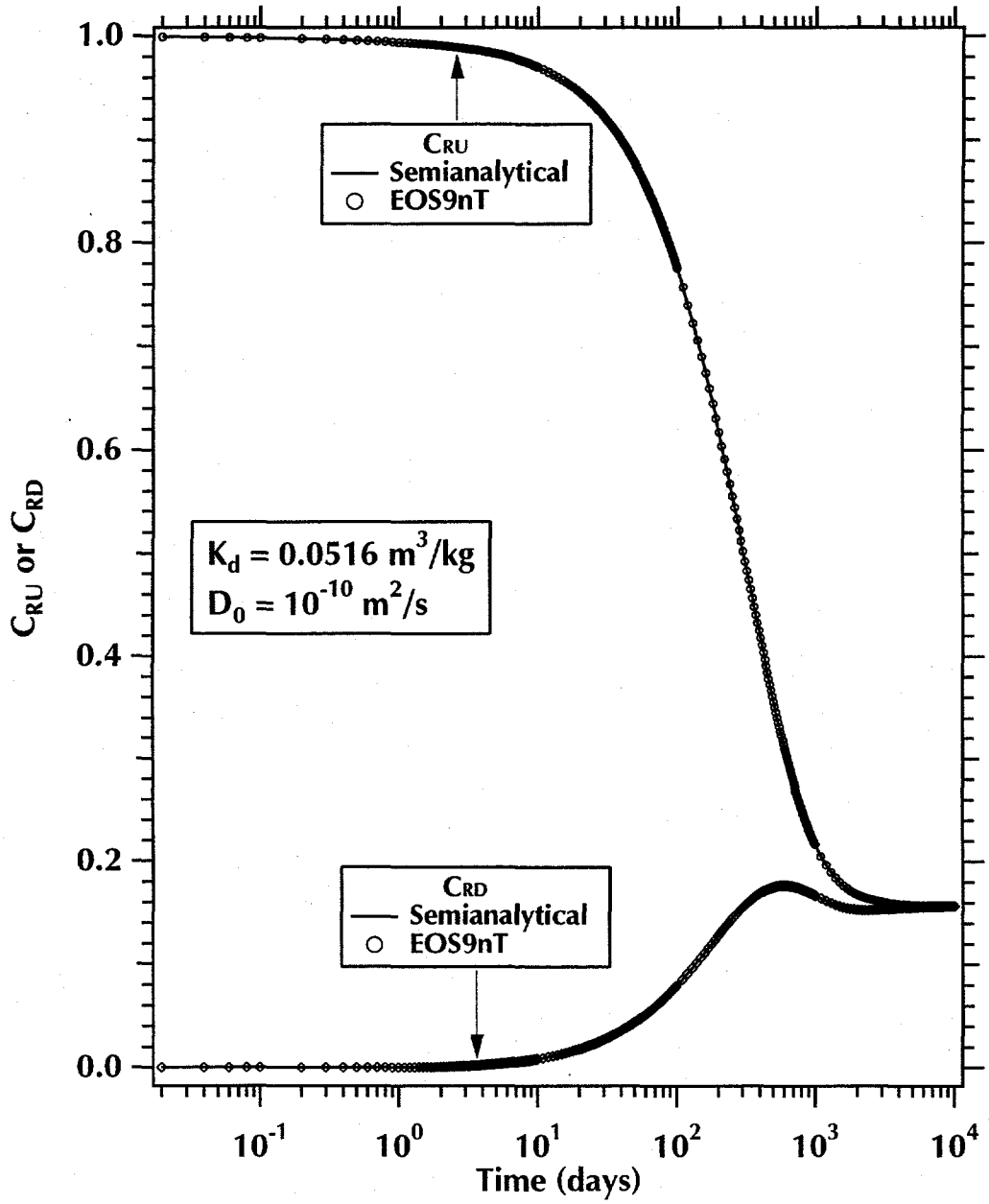

Figure 19. Semianalytical and EOS9nT solutions of the diffusion cell problem with kinetic sorption.

8.11. Test Problem 11

Sr-90 Diffusion at the H-Basin

The problem investigated here is that of Retention Basin 281-3H (hereafter referred to as the H-basin), a shallow catchment basin with permanently ponded water at the Savannah River Site (SRS) in South Carolina. The H-basin has been contaminated mainly by ^{137}Cs and ^{90}Sr. A detailed description of the pond, contamination, and the prevailing conditions at the site can be found in *Moridis et al.* [1996].

Moridis [1999] developed a semianalytical solution to determine the minimum extent (best-case scenario) of radionuclide transport and distribution. The actual transport is expected to be higher because of advection. Based on the basin geometry and thevolume of water in it, the cross-sectional area corresponding to each m^3 of water in the basin is 1.75 m^2. The soil in the H-basin area is mainly kaolinitic clay, which has limited ion-exchange capacity [*Moridis et al.*, 1996]. Batch sorption experiments showed that ^{90}Sr sorption is linear, with $K_d = 10^{-3}\ m^3/kg$ [*Hakem et al.*, 1997].

For this problem $\phi = 0.38$, $D_0 = 10^{-10}\ m^2 s^{-1}$, $V_U = 1\ m^3$, $A = 1.75\ m^2$, and we assume that the thickness of the medium $L = 100\ m$ (i.e., practically infinite). For ^{90}Sr, $T_{1/2} = 29.1$ years, corresponding to $\lambda = 7.5 \times 10^{-10}\ s^{-1}$. A complete description of the solution of this problem can be found in *Moridis* [1998].

The spatial distribution of the relative concentration of contaminants in the soil (with respect to initial concentration in the basin), C_{RP}, over time is shown in Figure 20, and indicates that at $t = 10^4$ days (roughly the time since the releases into the basin), the extent of contamination is limited to less than 1 m from the basin bottom and walls. Note that at $t = 10^5$ days, the contamination is limited to the top $3 - 3.5\ m$ from the contact area. The three EOS9nT solutions coincide, and are represented by a single symbol.

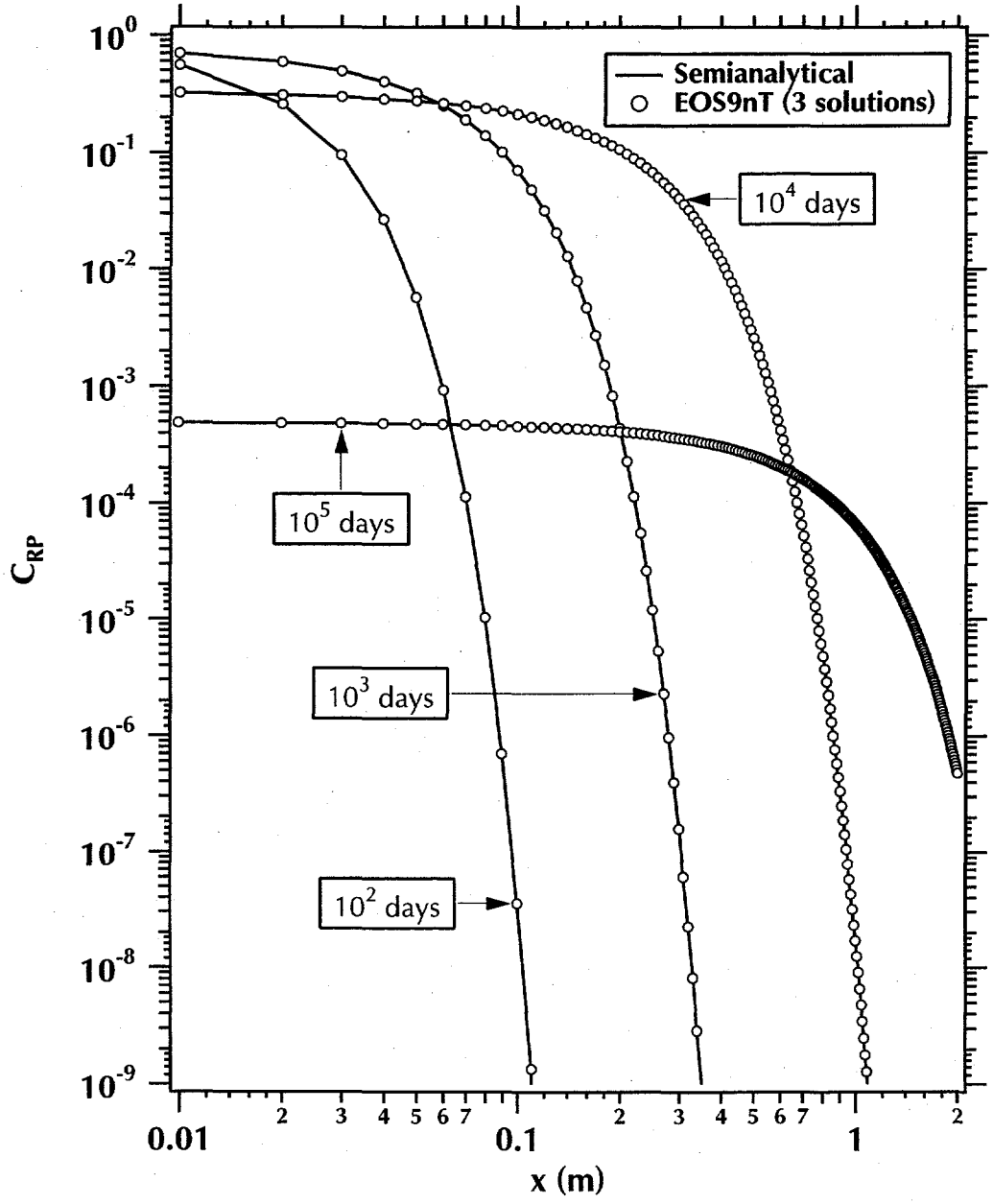

Figure 20. C_{RP} distribution over time in the porous medium of the H-basin example. Note that advection is neglected.

9. Summary and Conclusions

EOS9nT is a new TOUGH2 module for the simulation of flow and transport of an arbitrary number n of tracers (solutes and/or colloids) in the subsurface. The module first solves the Richards equation, which describes saturated or unsaturated water flow in subsurface formations. A second set of transport equations, corresponding to the n tracers/colloids, are then solved sequentially using the flow field information from the Richards equation. The very low concentrations of the n tracers are considered to have no effect on the density of the liquid phase, thus making possible the decoupling of the transport from the flow equations.

The n tracer transport equations account for sorption, radioactive decay, advection, hydrodynamic dispersion, molecular diffusion, filtration (for colloids only), first-order chemical reactions, and colloid-assisted tracer transport. A total of $n-1$ daughter products of radioactive decay can be tracked. EOS9nT can handle gridblocks of irregular geometry in 3-D domains, and offers the option of a Laplace space formulation of the transport equations (in additional to conventional timestepping) after the flow field becomes time-invariant. The

Laplace transform formulation eliminates the need for time discretization, and the problems stemming from the treatment of the time derivatives in the transport equations, and yields solutions semi-analytical in time.

We evaluated the performance of the EOS9nT module using a set of 11 1-D and 2-D test problems of flow and transport of solutes and colloids. Most of the test problems involved SC transport in fully saturated media under steady-state flow conditions, and have known analytical solutions. The test problem, which involved flow and SC transport in an unsaturated medium, has a known analytical solution of saturation distribution, but no analytical solution of the SC concentration.

Comparison between the analytical solutions and the 3 EOS9nT solutions (corresponding to conventional timestepping, and to the Stehfest and the De Hoog Laplace formulations) of the SC concentration distribution showed that in most cases practically coincided. The Stehfest algorithm uses real values for the Laplace space parameter s, is fast, powerful, and provides excellent results for $t \leq 1000$ years, but is not recommended for tracking of daughters of radioactive decay at any time. The De Hoog formulation uses complex values for s, quadruples the memory requirements, and is more computationally demanding, but allows an unlimited time step size without loss of accuracy for parents and duaghters.

An excellent agreement was observed between the analytical and numerical solutions of saturation in the unsaturated flow problem. In the same problem, the numerical results coincided with the numerical results obtained when using TOUGH2 with the EOS7R module [*Oldenburg and Pruess*, 1995], another module of flow and transport.

10. Acknowledgments

This work was supported by the Director, Office of Civilian Radioactive Waste Management, U.S. Department of Energy, through Memorandum Purchase Order EA9013MC5X between TRW Environmental Safety Systems and the Ernest Orlando Lawrence Berkeley National Laboratory (Berkeley Lab). The support is provided to Berkeley Lab through the U.S. Department of Energy Contract No. DE-AC03-76SF00098. Curt Oldenburg and Stefan Finsterle are thanked for their insightful review comments.

11. References

Bird, R.B., W.E. Stewart, and N.E.Lightfoot, *Transport Phenomena*, John Wiley, New York, 1960.

Bowen, D.D., and N. Epstein, Fine particle deposition in smooth parallel plate channels, *J. Colloid Interface Sci., 72*, 81-97, 1979.

Cameron, D.R., and A. Klute, Convective-dispersive solute transport with a combined equilibrium and kinetic adsorption model, *Water Resour. Res., 13*(1), 183-188, 1977.

Cho, C.M., Convective transport of ammonium with nitrification in soils, *Can. J. Soil Sci., 51*, 339-350, 1971.

Cleary, R.W., and M.J. Ungs, Groundwater pollution and hydrology, mathematical models and computer programs, *Report 78-WR-15*, Water Resour. Program, Princeton Univ., Princeton, N.J., 1978.

Çorapçioglu, M.Y., N.M. Abboud, and A. Haridas, Governing equations for particle transport in porous media, in *Advances in Transport Phenomena in Porous Media*, edited by : J. Bear and M.Y. Çorapçioglu, Series E: Applied Sciences Series No. 128, Martinus Nijhoff, Dordrecht, The Netherlands, 1987.

Cook, A. J., A desk study of surface diffusion and mass transport in clay, *Report WE/88/34*, Commission of the European Communities, Directorate-General, Sciences Research and Development, Louxemburg, 1989.

Crump, K. S., Numerical inversion of Laplace transforms using a Fourier Series approxi-

mation, *J. Assoc. Comput. Mach., 23*(1), 89-96, 1976.

De Hoog, F. R., J. H. Knight, and A.N. Stokes, An improved method for numerical inversion of Laplace transforms, *SIAM J. Sci. Stat. Comput., 3*(3), 357-366, 1982.

de Marsily, G., *Quantitative Hydrogeology*, Academic Press, San Diego, 1986.

Faure, G., *Principles of Isotope Geology*, John Wiley & Sons, New York, 1977.

Dieulin, J., Filtration de colloides d' actinides par une colonne de sable argileux, *Report LHM/RD/82/83*, Paris School of Mines, Fontainebleau, 1982.

Harada, M., P. L. Chambré, M. Foglia, K. Higashi, F. Iwamoto, D. Leung, D. H. Pigford, and D. Ting, Migration of radionuclides through sorbing media, *Report LBL-10500*, Lawrence Berkeley Laboratory, Berkeley, Calif., 1980.

Harvey, R.W., and S.P. Garabedian, Use of colloid filtration theory in modeling movement of bacteria through a contaminated sandy aquifer, *Env. Sci. Techn., 25*(1), 178-185, 1991.

Herzig, J.P., D.M. Leclerc, and P. Le Goff, Flow of suspension through porous media, *Ind. Eng. Chem., 62*, (5), 129-157, 1970.

Hiemenz, P.C., *Principles of Colloid and Surface Chemistry*, Marcel Dekker, New York, 1986.

Ibaraki, M.. Colloid-facilitated contaminant transport in discretely fractured media. Ph.D. thesis, Univ. of Waterloo, Waterloo, Ont., Canada, 1994.

Ibaraki, M., and E.A. Sudicky, Colloid-facilitated contaminant transport in discretely fractured media: 1. Numerical formulation and sensitivity analysis, *Water Resour. Res., 31*(12), 2945-2960, 1995.

Jahnke, F. M., Electrolyte diffusion in montmorillonite engineered barriers, Ph.D. dissertation, Univ. of Calif., Berkeley, 1986.

Jahnke, F. M., and C. J. Radke, Electrolyte diffusion in compacted montmorillonite engineered barriers, in *Coupled Processes Associated With Nuclear Waste Repositories*, pp. 287-297, Academic Press, Orlando, 1987.

James, S.C., and C.V. Chrysikopoulos, Transport of polydisperse colloid suspensions in a single fracture, *Water Resour. Res., 35*(3), 707-718, 1999.

Jensen, D. J., and C. J. Radke, Cation diffusion through compacted sodium montmorillonite at elevated temperature, *J. Soil Sci., 39*, 53-64, 1988.

Moridis, G. J., and D. L. Reddell, The Laplace Transform Finite Difference (LTFD) method for simulation of flow through porous media, *Water Resour. Res., 27*(8), 1873-1884, 1991.

Moridis, G. J., Alternative formulations of the Laplace Transform Boundary Element (LTBE) numerical method for the solution of diffusion-type equations, in *Boundary Element Technology VII*, pp. 815-833, Computational Mechanics Publications, Boston, and Elsevier Applied Science, New York, 1992.

Moridis, G.J, and K. Pruess, Flow and transport simulations using T2CG1, a package of conjugate gradient solvers for the TOUGH2 family of codes, *Report LBL-36235*, Lawrence Berkeley National Laboratory, Berkeley, Calif., 1995.

Moridis, G.J, and K. Pruess, T2SOLV: An enhanced package of solvers for the TOUGH2 family of reservoir simulation codes, *Geothermics, 27*(4), 415-444, 1998.

Moridis, G. J., Y.-S. Wu, and K. Pruess, EOS9nT: A TOUGH2 module for the simulation of flow and solute/colloid transport, *Report LBNL-41639*, Lawrence Berkeley National Laboratory, Berkeley, Calif., 1998.

Moridis, G. J., A set of semianalytical solutions for parameter estimation in diffusion cell experiments, *Report LBNL-41857*, Lawrence Berkeley National Laboratory, Berkeley, Calif., 1998 (also on the web at URL http://ccs.lbl.gov/Diffusion/).

Moridis, G. J., Semianalytical solutions for parameter estimation in diffusion cell experiments, *Water Resour. Res., 35*(6), 1729-1740, 1999.

Moridis, G.J, and G.S. Bodvarsson, Semianalytical solutions of radionuclide or reactive transport in layered fractured media, *Report LBL-44155*, Lawrence Berkeley National Laboratory, Berkeley, Calif., 1999.

Moridis, G. J., Y.-S. Wu, and K. Pruess, EOS3nT: A TOUGH2 module for nonisothermal fluid flow and solute/colloid transport, *Report LBNL-44260*, Lawrence Berkeley National Laboratory, Berkeley, Calif., 1999.

Oldenburg, C.M, and K. Pruess, EOS7R: Radionuclide transport for TOUGH2, *Report LBL-34868*, Lawrence Berkeley National Laboratory, Berkeley, Calif., 1995.

Pruess, K., TOUGH User's Guide, *Report LBL-20700*, Lawrence Berkeley National Laboratory, Berkeley, Calif., 1987.

Pruess, K., TOUGH2 - A general-purpose numerical simulator for multiphase fluid and heat flow, *Report LBL-29400*, Lawrence Berkeley National Laboratory, Berkeley, Calif., 1991.

Richards, L.A., Capillary conduction of liquids through porous mediums, *Physics, 1*, 318-333, 1931.

Saltelli, A., A. Avogadro, and G. Bidoglio, Americium filtration in glautonic sand columns, *Nucl. Technol., 67*, 245-254, 1984.

Skagius, K., and I. Neretnieks, Porosities and diffusivities of some nonsorbing species in crystalline rocks, *Water Resour. Res., 22*(3), 389-398, 1986.

Small, H., Hydrodynamic chromatogaphy: A technique for size analysis of colloidal particles, *J. Colloid Interface Sci., 48*(1),147-161, 1974.

Stehfest, H., Algorithm 368, Numerical inversion of Laplace transforms, *J. ACM, 13*(1), 47-49, 1970*a*.

Stehfest, H., Algorithm 368, Remark on algorithm 368 [D5], Numerical inversion of Laplace transforms, *J. ACM, 13*(1), 56, 1970*b*.

Tien, C., Turian, R.M. and Pendse, H.: 1979, Simulation of the dynamic behaviour of deep bed filters, *AICE J.* **25**(3), 385-395.

van der Lee, J., E. Ledoux, and G. de Marsily, Modeling of colloidal uranium transport in a fractured medium, *J. Hydrol., 139*, 135-158, 1992.

Wu, Y.S., C.F. Ahlers, P. Fraser, A. Simmons, and K. Pruess, Software qualification of selected TOUGH2 modules, *Rep. LBNL-39490*, Lawrence Berkeley National Laboratory, Berkeley, Calif., 1996.

Wnek, W.J., Gidaspow, D. and Wasan, D.T.: 1975, The role of colloid chemistry in modelling deep bed liquid filtration, *AICE J.* **25**(3), 385-395.

Wu, Y.S., and K. Mishra, Modifications and additions to selected TOUGH2 modules, *Rep. LBNL-41870*, Lawrence Berkeley National Laboratory, Berkeley, Calif., 1998.